Available online at www.sciencedirect.com
SCIENCE DIRECT
Coordination Chemistry Reviews 250 (2006) 424–448
COORDINATION CHEMISTRY REVIEWS
www.elsevier.com/locate/ccr

Review

Vibrational spectroscopy of phthalocyanine and naphthalocyanine in sandwich-type (na)phthalocyaninato and porphyrinato rare earth complexes

Jianzhuang Jiang [a,*], Meng Bao [a,b], Llew Rintoul [c], Dennis P. Arnold [c,**]

[a] *Key Laboratory for Colloid and Interface Chemistry of Education Ministry, Department of Chemistry, Shandong University, Jinan 250100, China*
[b] *Department of Chemistry, Jinan University, Jinan 250002, China*
[c] *School of Physical and Chemical Sciences, Queensland University of Technology, GPO Box 2434, Qld. 4001, Australia*

Received 3 March 2005; accepted 28 September 2005
Available online 2 November 2005

Contents

* Corresponding author.
** Corresponding author.

0010-8545/$ – see front matter © 2005 Elsevier B.V. All rights reserved.
doi:10.1016/j.ccr.2005.09.009

Abstract

This article reviews mainly the authors' efforts in studying and understanding the IR and Raman vibrational spectroscopic characteristics of (na)phthalocyanine in sandwich-type (na)phthalocyaninato and porphyrinato rare earth complexes. On the basis of systematic studies into the vibrational characteristics of (na)phthalocyanine in a wide range of homoleptic and heteroleptic bis- and tris-[(na)phthalocyaninato] and mixed (porphyrinato)[(na)phthalocyaninato] complexes of the whole series of rare earth metals, the effects of substituents, molecular symmetry, rare earth ionic size, rare earth valence state, and excitation wavelength on the vibrational characteristics of (na)phthalocyanine in sandwich rare earth complexes have been comparatively studied. The assignments of the IR and Raman bands of (na)phthalocyanine in these complexes have been made on the basis of comparison with related monomeric phthalocyanine compounds. Theoretical calculations of vibrational spectra for monomeric phthalocyanine derivatives are also helpful for the assignments. Both spectroscopic techniques reveal that the frequencies of pyrrole stretching, isoindole breathing, isoindole stretching vibrations, aza stretching vibrations, and coupling of pyrrole and aza stretching vibrations depend on the rare earth ionic size, shifting to higher energy along with the lanthanide contraction due to the increased ring–ring interaction across the series. Moreover, from the viewpoint of vibrational spectroscopy, the substitution of alkoxyl groups at the non-peripheral α positions of phthalocyanine rings exerts more influence on the intrinsic properties of phthalocyanines compared with substituents at peripheral β positions.
© 2005 Elsevier B.V. All rights reserved.

Keywords: Phthalocyanine; Porphyrin; Rare earth; Sandwich complex; IR spectra; Raman spectra

1. Introduction

Porphyrins and phthalocyanines are important classes of pigments that have fascinated chemists for many years due to their applications in various disciplines [1–3]. Both series can form complexes with almost the complete Periodic Table of elements. In particular, large metal ions such as rare earth, actinide, early transition, and main group metals form sandwich-type complexes with phthalocyanines and porphyrins [4–6].

Double-decker sandwich-type phthalocyaninato rare earth complexes have attracted great attention owing to their potential applications in materials science and molecular electronics and magnetism. The search for novel advanced molecular materials has stimulated intense research into substituted bis(phthalocyaninato) and bis(naphthalocyaninato), heteroleptic bis(phthalocyaninato), mixed (porphyrinato)(phthalocyaninato), and mixed (porphyrinato)(naphthalocyaninato) rare earth complexes especially since the beginning of the 1990s [4–6]. The wide range of applications arises from the specially intense π–π interaction between the conjugated tetrapyrrole ligands in these molecular materials. This recalls the crucial role played by proximate porphyrinoid pigments in photosynthesis and may lead to interesting molecular conductors. In this regard, rare earth porphyrinato or phthalocyaninato sandwich double-decker complexes are attractive models, and understanding their optical properties may provide insight into how the electronic properties of cofacial dimeric species influence the initial stages of the charge separation process.

Vibrational (IR and Raman) spectroscopy is a versatile technique for studying the intrinsic properties of the phthalocyanine compounds. In the past several years, we have carried out extensive and systematic studies into the vibrational (IR and Raman) characteristics of (na)phthalocyanine in a wide range of homoleptic and heteroleptic bis- and tris-[(na)phthalocyaninato] and mixed (porphyrinato)[(na)phthalocyaninato] complexes of the whole series of rare earth metals. This includes $M(Pc)_2$, $M[Pc(tBu)_4]_2$, $M[Pc(OC_8H_{17})_8]_2$, $M[Pc(\alpha\text{-}OC_5H_{11})_4]_2$, M(Pc)$[Pc(OC_8H_{17})_8]$, M(Pc)$[Pc(\alpha\text{-}OC_5H_{11})_4]$, $M[Nc(tBu)_4]_2$, $M[Nc(SC_{12}H_{25})_8]_2$, M(TClPP)(Pc), M(OEP)(Nc), M(TBPP)(Nc), and (Pc)M$[Pc(OC_8H_{17})_8]$M$[Pc(OC_8H_{17})_8]$ [M = Y, La–Lu except Pm, H_2Pc = unsubstituted phthalocyanine, $H_2Pc(tBu)_4$ = 2 (3), 9(10), 16 (17), 24(25) - tetra(*tert* - butyl)phthalocyanine, $H_2Pc(OC_8H_{17})_8$ = 2,3,9,10,16,17,24,25-octakis(octyloxy)phthalocyanine, $H_2Pc(\alpha\text{-}OC_5H_{11})_4$ = 1,8,15,22-tetrakis(3-pentyloxy)phthalocyanine, $H_2Nc(tBu)_4$ = 3(4),12(13),21(22),30(31)-tetrakis(*t*-butyl)-2,3-naphthalocyanine, $H_2Nc(SC_{12}H_{25})_8$ = 3,4,12,13,21,22,30,31-octa(dodecylthio)-2,3-naphthalocyanine, H_2TClPP = 5,10,15,20-tetra(4-chloro)phenylporphyrin, H_2OEP = 2,3,7,8,12,13,7,18-octaethylporphyrin, H_2TBPP = 5,10,15,20-tetra(4-*t*-butyl)phenylporphyrin] [7–20] (Fig. 1) and our work follows the precedent studies of Aroca, Homborg, and Tran-Thi [21–38]. To benefit the assignments of vibrational modes in the experimental spectra, we have also calculated from theory the vibrational characteristics of monomeric phthalocyanine derivatives [39–41].

Despite the existence of a large number of reports on the topic of phthalocyanine vibrational characteristics accumulated in the past several decades, there has been no review article that systematically generalizes the research achievements in this field. In this review, we seek to summarize our research results on the IR and Raman vibrational characteristics of (na)phthalocyanine compounds, in particular in various kinds of sandwich-type rare earth complexes. We hope that this compilation of the vibrational properties of (na)phthalocyanine in these fascinating sandwich-type rare earth complexes will interest many scientists in both industrial and theoretical fields.

2. Experimental techniques

The various series of homoleptic and heteroleptic bis(phthalocyaninato) and tris(phthalocyaninato), homoleptic bis(naphthalocyaninato), mixed (porphyrinato)(phthalocyaninato), and mixed (porphyrinato)(naphthalocyaninato) rare earth complexes were prepared according to published procedures [42–66]. Their sandwich nature has been well established through elemental analysis, a range of spectroscopic methods,

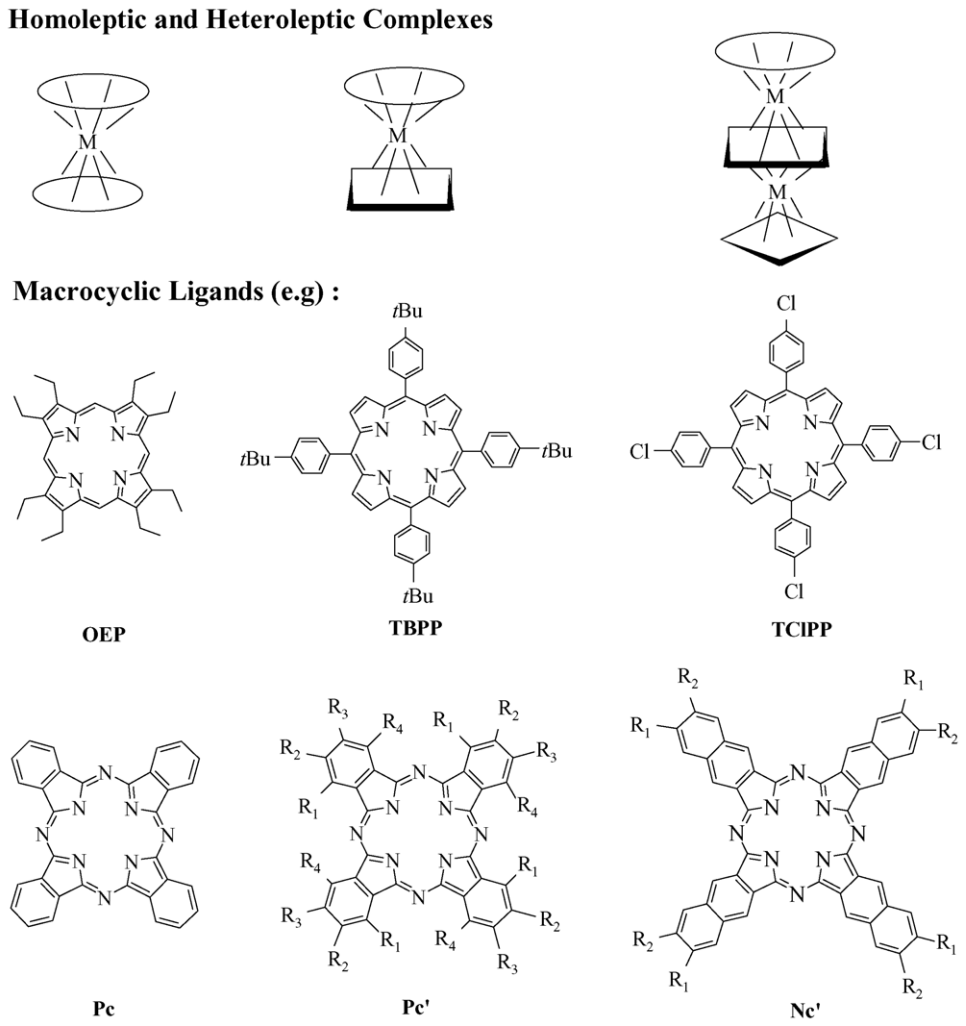

Fig. 1. The schematic molecular structures of homoleptic and heteroleptic bis(phthalocyaninato), bis(naphthalocyaninato), tris(phthalocyaninato), mixed (porphyrinato)(phthalocyaninato), and mixed (porphyrinato)(naphthalocyaninato) rare earth complexes and the structures of the macrocyclic ligands.

and single crystal X-ray diffraction. In our work, IR spectra were recorded in KBr pellets with 2 cm^{-1} resolution using a BIORAD FTS-165 spectrometer. Resonance Raman spectra were recorded on a few grains of the solid samples with ca. 4 cm^{-1} resolution using a Renishaw Raman Microprobe, equipped with a Spectra Physics Model 127 He–Ne laser excitation source emitting at a wavelength of 632.8 nm, and a Renishaw diode laser emitting at 785 nm, and a cooled charge-coupled device (CCD) camera. An Olympus BHZ-UHA microscope fitted with three objective lenses ($\times$10, $\times$20, $\times$50) was attached, and we use the $\times$10 objective, which gives a spot size on the sample of about 5 μm. Laser power at the sample is approximately 0.08 mW. This technique is very convenient, and unless the sample is particularly prone to fluorescence, spectra of excellent quality are obtainable in approximately 3 min.

3. Molecular structures and molecular symmetry

First we present a brief description of the molecular structures and symmetry properties of the various kinds of sandwich-type (na)phthalocyaninato and porphyrinato rare earth complexes, especially the (na)phthalocyaninato-metal fragment, because of the close relationship between the vibrational properties and molecular symmetry.

According to the single crystal X-ray diffraction structural analyses of unsubstituted and substituted homoleptic bis(phthalocyaninato) rare earth complexes $M(Pc)_2$ (M = Y, La, Ce, Pr, Nd, Er, Lu), $Lu[Pc(SC_6H_{13})_8]_2$ [$Pc(SC_6H_{13})_8$ = 2,3,9,10,16,17,24,25-octakis(hexylthio)phthalocyanine], and $Yb[Pc(15C5)_4]_2$ [4,67,68], their static symmetry is D_4 or D_{4d} depending on the twist (skew) angle between the two macrocyclic rings, which ranges from 38° to 45°. For the non-structurally characterized homoleptic rare earth complexes $M[Pc(OC_8H_{17})_8]_2$, D_4 or D_{4d} group symmetry is also reasonably assumed due to the symmetrical location of eight octyloxy groups on the phthalocyaninato rings. For $M[Pc(tBu)_4]_2$, the actual samples contain more than one isomer due to the random location of the four *tert*-butyl groups, leading to lower symmetry. This is clearly revealed by the larger number of vibrational modes observed in the IR and Raman spectra of $M[Pc(tBu)_4]_2$ compared with those of $M(Pc)_2$ and $M[Pc(OC_8H_{17})_8]_2$ [9,19].

The homoleptic bis(phthalocyaninato) rare earth complexes $M[Pc(\alpha\text{-}OC_5H_{11})_4]_2$ were prepared according to the published procedure [69a]. However, due to the C_{4h} symmetry of the $Pc(\alpha\text{-}OC_5H_{11})_4$ ligand and the double-decker structure, a mixture of two stereoisomers having S_8 and D_4 symmetry was actually obtained. The former isomer, which is the major product, can be separated by recrystallization due to its higher crystallinity and the IR and Raman spectroscopic characteristics of the series of S_8 isomers have been studied. According to the molecular structure of the bis(phthalocyaninato) yttrium complex $Y[Pc(\alpha\text{-}OC_5H_{11})_4]_2$, the static symmetry of these double-decker molecules in the solid state is S_8 [69a].

There is also no crystallographic report on the molecular structure of heteroleptic bis(phthalocyaninato) rare earth compounds containing peripherally octa(alkoxy)-substituted phthalocyanine ligand. However, according to the recent work on the molecular structure of 2,3,9,10,16,17,24,25-tetrakis(15-crown-5)phthalocyanine-containing heteroleptic bis(phthalocyaninato) europium compound $Eu(Pc)[Pc(15C5)_4]$ [$H_2Pc(15C5)_4$ = 2,3,9,10,16,17,24,25-tetrakis(15-crown-5)phthalocyanine] [69b], the skew angle between the two phthalocyanine macrocyclic ligands is very close to 45°. The equilibrium geometry of $Eu(Pc)[Pc(15C5)_4]$ is therefore C_{4v}. This should also be true for the alkoxy-substituted analogues $M(Pc)[Pc(OC_8H_{17})_8]$. Structurally characterized heteroleptic bis(phthalocyaninato) rare earth compounds containing non-peripherally substituted 1,8,15,22-tetrakis(3-pentyloxy)phthalocyanine ligand including $M(Pc)[Pc(\alpha\text{-}OC_5H_{11})_4]$ (M = Sm, Eu, Er) were also reported very recently by Jiang and co-workers [53,54]. According to the X-ray molecular structure analysis results, the equilibrium geometry of $M(Pc)[Pc(\alpha\text{-}OC_5H_{11})_4]$ has C_4 point group symmetry. Molecular symmetry lower than D_4 or D_{4d} for heteroleptic bis(phthalocyaninato) rare earth complexes $M(Pc)[Pc(OC_8H_{17})_8]$ and $M(Pc)[Pc(\alpha\text{-}OC_5H_{11})_4]$ has been verified by their complicated IR and Raman spectra in comparison with those of homoleptic counterparts $M(Pc)_2$ and $M[Pc(OC_8H_{17})_8]_2$ [7,9,11,17].

To assist the interpretation of the observed IR and Raman vibrational spectra of above-mentioned homoleptic and heteroleptic bis(phthalocyaninato) rare earth complexes, local C_{4v} symmetry for the fragment M(Pc) and $M[Pc(OC_8H_{17})_8]$ in $M(Pc)_2$, $M[Pc(OC_8H_{17})_8]_2$, $M(Pc)[Pc(OC_8H_{17})_8]$, and C_4 for $M[Pc(\alpha\text{-}OC_5H_{11})_4]$ in $M(Pc)[Pc(\alpha\text{-}OC_5H_{11})_4]$ and $M[Pc(\alpha\text{-}OC_5H_{11})_4]_2$ (S_8 isomer), is reasonably assumed [9,11,17,19,20].

The C_{4v} symmetrical unsubstituted phthalocyanine metal fragment M(Pc) contains 57 atoms, so there are 63 IR-active and 105 Raman-active modes among the 165 total normal vibrational modes. There are only $22A_1$ totally symmetric fundamental vibrations active in the spontaneous Raman spectra, although the fragment M(Pc) contains a large number of atoms and thus possesses many possible normal vibrational modes. In the resonance Raman scattering, a number of new frequencies could be attributed to the related $22B_1$, $20B_2$, and 41E type in view of the Herzberg–Teller mechanism. The vibrational modes for the fragment M(Pc) with C_{4v} symmetry may be summarized as follows, where "IR" and "R" represent Infrared- and Raman-active modes, respectively.

$$\Gamma_{vib} = 22A_1\,(IR, R) + 19A_2 + 22B_1\,(R) + 20B_2\,(R) + 41E\,(IR, R)$$

A_1 and E modes are both IR- and Raman-active. B_1 and B_2 modes are Raman-active and A_2 modes are vibrationally inactive. On the other hand, for the corresponding 57-atom fragment with C_4 symmetry, there are 70 IR-active and 81 Raman-active modes that dominate the IR and Raman spectra among the 165 total normal vibrational modes.

Similar to $Zr[Pc(tBu)_4]_2$ [22,23], only frequencies corresponding to the characteristic fingerprint vibrations of the Pc macrocycle are observed and the alkyloxy or alkyl substituent vibrations are very weak or absent in the Raman spectra of $M[Pc(OC_8H_{17})_8]_2$, $M[Pc(\alpha\text{-}OC_5H_{11})_4]_2$, $M(Pc)[Pc(OC_8H_{17})_8]$, $M(Pc)[Pc(\alpha\text{-}OC_5H_{11})_4]$, $M[Pc(tBu)_4]_2$. Thus, the octyloxy, 3-pentyloxy, and *tert*-butyl groups will be ignored in our subsequent analysis of their Raman spectra. However, this rule cannot be applied for their IR spectroscopy. The presence of eight octyloxy, four 3-pentyloxy, and four *tert*-butyl groups on the peripheral and non-peripheral position of one or two phthalocyanine ring(s) in homoleptic double-decker molecules $M[Pc(OC_8H_{17})_8]_2$, $M[Pc(\alpha\text{-}OC_5H_{11})_4]_2$, $M[Pc(tBu)_4]_2$, and heteroleptic double-decker molecules of $M(Pc)[Pc(OC_8H_{17})_8]$ and $M(Pc)[Pc(\alpha\text{-}OC_5H_{11})_4]$ increases the number of IR-active modes. This is also true for $M[Nc(tBu)_4]_2$.

According to the sole report on the crystal structure of homoleptic tris(phthalocyaninato) lutetium complex $Lu_2[Pc(15C5)_4]_3$ [70], the static symmetry of the triple-decker is approximately D_{4h} because of the symmetrical molecular structure and the nearly 45° twist angle between the outer and inner macrocyclic rings. The D_{4h} molecular symmetry is also assumed in the heteroleptic tris(phthalocyaninato) rare earth complexes $(Pc)M[Pc(OC_8H_{17})_8]M'(Pc)$ (M = or ≠ M′ = Er, Lu) for the same reason [63]. For heteroleptic tris(phthalocyaninato) rare earth analogues $(Pc)M[Pc(OC_8H_{17})_8]M[Pc(OC_8H_{17})_8]$, relatively lower group symmetry than D_{4h}, say C_{4v}, is reasonably assumed due to the presence of eight octyloxy groups on two neighbouring phthalocyanine rings of the three in the molecule. This is verified by the complicated IR spectra of this series of heteroleptic tris(phthalocyaninato) rare earth complexes compared with those of $M(Pc)_2$ and $M[Pc(OC_8H_{17})_8]_2$ [9,10]. As for the bis(phthalocyaninato) rare earth analogues, to assist in the interpretation of the observed IR spectra of $(Pc)M[Pc(OC_8H_{17})_8]M[Pc(OC_8H_{17})_8]$, a local C_{4v} symmetry for each phthalocyanine ring together with one central rare earth metal atom is assumed.

The Raman spectra of the mixed (porphyrinato)(phthalocyaninato) double-decker compounds of rare earth metals M(TClPP)(Pc) (M = Y, La–Lu except Pm) are dominated by the phthalocyanine ligand modes when exciting laser lines of 633, 780, and 1064 nm are employed [13,18,38]. This is because the phthalocyanine Q absorption bands located near 670 nm are in closer resonance with these laser sources than are the porphyrin Q bands at ca. 550 nm, and the latter are only one-tenth as strong as the former. This is also true for the mixed (porphyri-

nato)(naphthalocyaninato) double-deckers M(Por)(Nc) (M = Y, La–Lu except Ce; Por = OEP, TBPP) [15,16]. Good correspondence in the Raman features between $M(Pc)_2$ and corresponding M(TClPP)(Pc), and between $M[Nc(tBu)_4]_2$ and M(Por)(Nc) (Por = OEP, TBPP) provides more direct evidence that the Raman spectra of M(TClPP)(Pc) and M(Por)(Nc) (Por = OEP, TBPP) are dominated by the phthalocyaninato- and naphthalocyaninato-metal fragment M(Pc) and M(Nc), respectively. The static molecular geometry of M(TClPP)(Pc) and M(OEP)(Nc) suggests a C_{4v} point group for both the whole molecule and the fragment M(Pc) and M(Nc) in the mixed ring double-deckers [15,16,18]. Even the unsubstituted naphthalocyaninato-metal fragment with 81 atoms and 237 normal vibrational modes is a tremendous challenge for the vibrational spectroscopist. For a C_{4v} M(Nc) fragment, there will be only $31A_1$ totally symmetric modes that dominate the spontaneous Raman spectra. The other Raman-active modes include $30B_1$, $30B_2$, and 118E, which will show a number of new frequencies in the resonance Raman scattering in view of the Herzberg–Teller mechanism. Despite the large number of fundamental vibrational modes, the Raman spectra of these mixed ring double-decker complexes are composed of a small number of bands [15,16]. For a C_{4v} M(Nc) fragment there will be $31A_1$ and 118E IR active modes that dominate the IR spectra.

There has been no crystallographic report on the molecular structure of bis(naphthalocyaninato) metal complexes. However, according to the molecular structures of mixed (octaethylporphyrinato)(naphthalocyaninato) rare earth double-deckers M(OEP)(Nc) (M = Y, La–Lu except Pm), the skew angles between OEP and Nc macrocyclic ligands in the whole series of rare earth compounds remain unchanged at 45° in order to minimize the non-bonding interactions between the fused benzene rings of Nc and the β-ethyl groups of OEP [55,57,58]. Therefore, it is reasonable to assume that the skew angle between two Nc rings in $M[Nc(tBu)_4]_2$ and $M[Nc(SC_{12}H_{25})_8]_2$ is nearly 45°. The equilibrium structures of $M[Nc(tBu)_4]_2$ and $M[Nc(SC_{12}H_{25})_8]_2$ should have D_{4d} group symmetry when the skew angle is 45° or D_4 when the skew angle slightly deviates from 45°. Similar to $M[Pc(tBu)_4]_2$ (M = Zr, rare earth), the actual samples of $M[Nc(tBu)_4]_2$ contain more than one isomer due to the random location of the *tert*-butyl groups. However, for each substituted Nc ring and the central rare earth metal atom, a local C_{4v} symmetry should be seen and the interpretation of the observed vibrational spectra could be assisted by this approximation. As in the Raman spectra of $M[Pc(tBu)_4]_2$, only frequencies corresponding to the characteristic fingerprint vibrations of the Nc macrocycle were observed and *tert*-butyl vibrations were very weak or absent [14]. This is also because both laser lines (633 and 780 or 785 nm) used in our experiments appear to enhance modes associated with the aromatic macrocycles. The situation is also true for $M[Nc(SC_{12}H_{25})_8]_2$ [8].

4. IR spectroscopic properties

Based on their detailed studies on the vibrational spectra of both phthalocyanine and naphthalocyanine compounds, Aroca and co-workers found that the following three groups of characteristic phthalocyanine or naphthalocyanine vibrations dominate their IR and Raman spectra [21–24]. In the spectral region from 400 to 1000 cm^{-1}, the vibrations are mainly composed of the dihedral plane deformations involving the aromatic C–H groups (wagging and torsion vibration) that are normally seen in the IR spectra, and ring radial vibrations of the isoindole moieties and the macrocycle that show strong Raman signals. Aromatic in-plane C–H vibrations are responsible for the IR and resonance Raman spectra of phthalocyanine molecules in the region of 1000–1300 cm^{-1}, with the exception of the pyrrole ring vibration at about 1140 cm^{-1}. Vibrational frequencies in the range of 1300–1650 cm^{-1} are derived from isoindole ring stretches and the C=N aza group stretch, from which the pyrrole stretching vibrations at ca. 1330 and 1510 cm^{-1}, and *ortho*-substituted benzene (or naphthalene) stretching vibrations at ca. 1560, 1590, and 1610 cm^{-1} or above can be distinguished by frequency and relative intensity.

4.1. IR spectra of $M(Pc)_2$ [9]

Fig. 2 compares the IR spectra in the region of fundamental frequencies of 400–1800 cm^{-1} of three compounds $M(Pc)_2$ (M = Nd, Tb, Lu) with resolution of 2 cm^{-1}, typical for the light, middle, and heavy rare earths, respectively, as well as the spectrum of the unique $Ce(Pc)_2$ complex. In Table 1, characteristic IR vibrational frequencies of the phthalocyanine ligand in bis(phthalocyaninato) compounds of the whole series of lanthanides are summarized. Their interpretation is derived by analogy with the IR and Raman characteristics of some previously reported $M(Pc)_2$ [21–24] and the vibrational properties of metal free phthalocyanine [71], with assistance from our recent theoretical research into the vibrational spectra of monomeric phthalocyanine derivatives [39–41]. The characteristic frequency approximation is necessary in dealing with the observed vibrational frequencies for such a large conjugated system, where only a handful of vibrational modes can be given an assignment in terms of internal coordinates, as exemplified in Table 1.

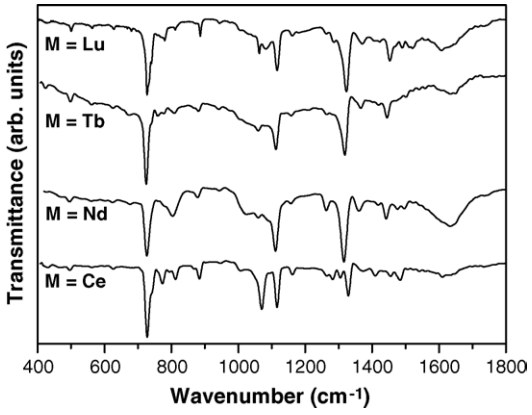

Fig. 2. IR spectra of $M(Pc)_2$ (M = Ce, Nd, Tb, Lu) in the region of 400–1800 cm^{-1} recorded in KBr pellets.

Table 1
Characteristic IR bands (cm^{-1}) of phthalocyanine for $M(Pc)_2$

La	Ce	Pr	Nd	Sm	Eu	Gd	Tb	Dy	Y	Ho	Er	Tm	Yb	Lu	Assignment
422w	432w	429w	425w	427w	427w	419w	425w	426w	425w	427w	425w	425w	426w	427w	
492w	497w	493w	496w	498w	498w	498w	499w	500w	499w	500w	500w	500w	500w	501w	
558w	562w	573w	560w	560w	561w	561w	561w	562w	561w	562w	560w	561w	562w	592w	
620w	626w	624w	624w	625w	625w	625w	625w	626w	625w	626w	625w	625w	626w	628w	Pc breathing
682w	674w	675w	676w	678w	676w	675w	674w	678w	671w	679w	679w	680w	680w	680w	Pc breathing
729s	727s	724s	726s	727s	727s	724s	724s	726s	725s	728s	725s	726s	729s	727s	C–H wag
742w	740w	739w				739m	740w	739w	740w		739m			741w	C–H wag
753w		757w	761w	758w	760w	761w	763w	758w	762w	760w	756w	761w	758w	758w	Pc ring
765w	772m	780w	780w	782w	778w	777w	778w	779w	777w	779w	780w	775w	779w	780w	
808w	812m	806w	803m	809w	809w	810w	808w	810w	808w	810w	809w	809w	812w	811w	
876m	884m	877w	879w	881m	881w	881m	881w	884w	883w	884w	884w	884w	885w	887m	Coupling of isoindole deformation and aza stretching
946w	946w	943w	943w	944w	944w	941w	941w	943w	942w	942w	942w	942w	945w	943w	
1007m	1007w	1003w	1002w	1006w	1005w	1000w	1004w	1004w			1002w	1003w	1005w	1009w	Pyrrole-N in-plane bending
1059w	1070s	1057w	1059w	1060w	1061w	1060w	1060w	1062w	1062w	1063w	1062w	1063w	1064w	1062w	Coupling of isoindole deformation and aza stretching
1095w	1094w	1075w	1091w	1084w	1083w	1080w	1080w			1097w		1087w	1086w	1083w	C–H bend
1110s	1116s	1108s	1111s	1113s	1113s	1113s	1112s	1115s	1114s	1115s	1114s	1115s	1116s	1116s	Isoindole breathing
1143w		1136w		1140w	1140w	1138w	1136w	1137w				1140w			Pyrrole breathing
1158w	1162w	1156w	1157w	1161w	1159w	1160w	1158w	1160w	1160s	1159w	1160w	1160w	1159w	1161w	C–H bend
	1201w	1211w		1202w	1212w	1208w	1210w	1203w	1199w		1213w	1204w			
1264w	1266w	1238w	1264w	1264w	1264w	1245w	1264w	1263w	1264w	1262w	1264w	1267w	1264w	1264w	C–H bend
1281w	1282w	1266w		1283w	1284w	1283w	1284w	1283w	1284w	1281w	1283w	1283w	1282w	1287w	C–H bend
1313s	1306w	1312s	1316s	1318s	1319s	1319s	1319s	1320s	1320s	1321s	1320s	1320s	1322s	1323s	Pyrrole stretching
	1329m														Pyrrole stretching
1353w	1373w	1352m	1367w	1370m	1366m	1367w	1367w	1369m	1370w	1370w	1370w	1371w	1372w	1371w	Isoindole stretching
1399w		1397m	1399w	1400w	1400m	1386w	1388w	1401w	1402w	1405w	1385w	1403w	1404w	1407w	
1419w	1410w	1419w	1419w	1420w	1419w	1422w	1420w	1422w	1422w	1422w	1421w	1421w	1424w	1423w	Isoindole stretching
1439m	1433w	1438m	1442m	1444m	1445m	1444m	1445m	1448m	1448m	1450m	1448m	1450m	1453m	1454m	Isoindole stretching
1475m	1455w	1474w	1476w	1481w	1482w	1478w	1472w				1472w	1471w	1471w	1467w	Isoindole stretching
1492w	1484m	1491w						1486w	1487w	1488w	1489w	1490w	1490w	1490w	Isoindole stretching
1506w	1506w		1496w	1499w	1501w	1502w	1500w	1504w	1505w	1505w	1506w	1508w	1509w	1512w	Coupling of pyrrole and aza stretching
1522w	1522w	1523w	1523w	1522w	1521w	1521w	1522w	1522w	1523w	1523w	1523w	1521w		1521w	Aza stretching
1541w	1541w	1543w	1541w	1541w	1543w	1543w	1540w	1541w	1542w	1541w	1542w	1542w	1541w		Benzene stretching
1558w	1559w	1559w	1561w	1561w	1558w	1558w	1559w	1559w	1560w	1559w	1559w	1559w	1559w	1557w	Benzene stretching
1620w	1610w	1607w		1608w	1609w	1610w		1608w	1607w	1608w	1606w		1606w	1609w	Benzene stretching
1634w	1635w	1634w	1633m	1634w	1634w	1634m	1635w	1636m	1635w	1635w	1636m	1636m	1633w		Benzene stretching
1650m		1646w		1647w	1698w	1649w	1649w		1650w	1645w		1648m	1650w	1647w	Benzene stretching
3044w	3039w	3033w	3057w	3050w	3051w	3038w	3047w	3057w	3053w	3050w	3056w	3051w	3051w	3052w	C–H stretching
3079w	3165w	3096w	3112w	3113w	3078w	3076w	3102w	3078w	3107w	3077w	3104w	3182w	3147w	3076w	C–H stretching

The simple patterns of the infrared spectra of unsubstituted bis(phthalocyaninato) rare earth complexes $M(Pc)_2$ (M = Y, La–Lu except Ce and Pm) closely resemble the previously published results on $M(Pc)_2$ in some scattered reports (M = Y, La, Pr, Nd, Gd, Dy, Ho, Yb, Lu) [21–29,36,37,72]. Due to the similar molecular structure among the whole series of bis(phthalocyaninato) lanthanide compounds, all these compounds show similar IR characteristics. Four main IR absorptions corresponding to the C–H wagging at ca. 730 cm^{-1}, isoindole breathing and C–H bending coupled at 1110–1116 cm^{-1}, pyrrole stretching at 1312–1323 cm^{-1}, and isoindole stretching at 1439–1454 cm^{-1} have been found to dominate the IR spectra of $M^{III}(Pc)_2$. Among these, the most intense pyrrole stretching absorption at 1312–1323 cm^{-1} is assigned to the IR marker band of phthalocyanine monoanion-radical $Pc^{\bullet -}$ by comparison between the IR characteristics of $M^{III}(Pc)_2$ and $[NBu_4][M(Pc)_2]$ [73], according to the work of Kadish et al. [74,75]. In the region from 400 to 1000 cm^{-1}, the remaining weak vibrations have principal contributions from the dihedral plane deformation involving the aromatic C–H groups (wagging, torsion, and out-of-plane bending vibrations). Aromatic in-plane C–H bending vibrations are responsible for the IR bands of phthalocyanine molecules in the region of 1000–1300 cm^{-1}, with the exception of the band at about 1140 cm^{-1} due to the pyrrole ring breathing, at 1110–1116 cm^{-1} mainly contributed from isoindole breathing together with some C–H bending, and the weak band at 1057–1064 cm^{-1} due to the coupling of isoindole deformation and aza stretching. Vibrational frequencies in the range of 1300–1650 cm^{-1} are derived from pyrrole stretch, benzene stretch, isoindole ring stretch, and the aza group stretch, for which the pyrrole stretching vibrations appear at 1312–1323 cm^{-1}. Another pyrrole stretching-related vibration couples with the aza stretching and appears at ca. 1510 cm^{-1}. The *ortho*-substituted benzene stretching vibrations are observed at ca. 1610 cm^{-1}. The weak band at 1352–1372 cm^{-1} is assigned to the isoindole stretching vibration because of its sensitivity to the rare earth ionic size as summarized in Table 1. A weak band around 3050 cm^{-1} is due to the aromatic C–H stretching vibrations on the phthalocyanine rings [21–29,36,37,72].

In describing the IR characteristics of naphthalocyanine in $M[Nc(tBu)_4]_2$ [8], we raised a question concerning the origin of the appearance of two pyrrole stretching absorptions at 1314–1317 and 1323–1330 cm^{-1} for $M[Nc(tBu)_4]_2$. The presence of only one absorption band in the same region for analogues $M[Nc(SC_{12}H_{25})_8]_2$ under the same conditions appears to suggest that this is due to the decreased symmetry of the $M[Nc(tBu)_4]_2$ molecules. The fact that only one band at 1312–1323 cm^{-1} is observed for the whole series of tervalent rare earth bis(phthalocyaninato) complexes $M(Pc)_2$ suggests that this explanation is correct. The vibrations at 1312–1323 cm^{-1} attributed to pyrrole stretching vibrations and at 1439–1454 cm^{-1} due to the isoindole stretching in the IR spectra of $M(Pc)_2$ shift slightly and linearly to higher energy along with the decrease of rare earth radius, clearly showing the rare earth size effect. Not only the frequency but also the absorption intensity of these vibrations, especially of the former one, show dependence on the rare earth ionic size. Along with the decrease of rare earth radius, the pyrrole stretching vibrations at 1312–1323 cm^{-1} gradually lose some intensity. This is the reason that the most intense absorption band is one of pyrrole stretching vibrations appearing at 1312–1319 cm^{-1} for the light rare earth to middle rare earth bis(phthalocyaninato) compounds, while for heavy rare earth analogues this vibration appears as the second most intense absorption band at 1321–1323 cm^{-1} and the most intense one locates at 728 cm^{-1} due to the C–H wagging vibrations. In addition, the weak vibrational band at 876–887 cm^{-1} in the IR spectra of bis(phthalocyaninato) rare earths has also been found to be sensitive to the central rare earth size. This is in line with the result of Isago and Shimoda on the IR investigation of several bis(phthalocyaninato) rare earth compounds $M(Pc)_2$ (M = La, Pr, Sm, Eu, Tb, Ho, Yb) [76]. However, the assignment of this vibrational mode has been the subject of some controversy. Considering the location of this absorption frequency, Aroca and co-workers assigned it to the C–H wagging of the Pc ring [21,25,27]. On the basis of the metal-sensitive nature of the band at ca. 880 cm^{-1}, Isago attributed this band to the rare earth metal–nitrogen (pyrrole) vibration following the assignment for monomeric phthalocyaninato-metal complexes by Kobayashi et al. [77] and Kenn and Malerbi [78]. The metal-sensitive nature of this vibration revealed by our systematic research clearly excludes the attribution of this absorption to a C–H wagging-only mode. According to our recent results on the vibrational properties of H_2Pc calculated at density functional B3LYP level using the 3-21G basis set [39–41], this absorption band is found to have primary contributions from the isoindole deformation and aza vibration, as assigned in Table 1. Another metal-sensitive vibration mode at 1110–1116 cm^{-1} is also noteworthy. This intense absorption that was previously assigned to the C–H bending-only mode, is now re-assigned mainly to the isoindole breathing with some C–H in-plane bending contribution, also according to our theoretical research [39–41]. In conclusion, all the rare earth size-dependent IR absorptions of phthalocyanine in bis(phthalocyaninato) rare earth complexes should be contributed primarily from the vibrations of pyrrole, or isoindole stretching, breathing or deformation or aza stretching involving the pyrrole or aza nitrogen atoms. This logical conclusion is reinforced by the molecular structural studies of a series of tetrapyrrole metal double-deckers, as distortion of the two rings (Por and Pc or Nc) arises mainly from the tilting of sub-units using the bridging atoms (aza N for Pc or Nc, *meso* CH carbon atoms for Por) as hinge joints, which makes the two ligands significantly domed [58,73]. The degree of the distortion (doming) of each tetrapyrrole ligand is directly dependent on the size of the metal sandwiched between the two tetrapyrrole rings, which in turn induces systematic frequency changes in the corresponding vibrational modes involving the pyrrole and aza nitrogen atoms, namely pyrrole or isoindole breathing, stretching and deformation, and aza stretching.

As shown in Table 1, the IR characteristics of phthalocyanine dianion Pc^{2-} could not be distinguished in the IR spectra of $M^{III}(Pc)_2$ and thus IR spectra of bis(phthalocyaninato) rare earth(III) complexes can be attributed solely to the phthalo-

cyanine monoanion radical $Pc^{\bullet -}$. This clearly verifies that the unpaired electron delocalizes over the two phthalocyanine macrocycles on the IR time scale, which accords well with the result deduced from the Raman spectra of the same compounds [19] and the IR and Raman spectra of bis(naphthalocyaninato) rare earth counterparts [8].

Among the whole series of bis(phthalocyaninato) rare earth complexes, the cerium double-decker is particularly interesting. As indicated from the electronic absorption, Raman, ^{1}H NMR, XNAFS, and electrochemical studies [62], both phthalocyanine rings exist as dianions in bis(phthalocyaninato)cerium $Ce(Pc^{2-})_2$. This is despite the expectation of an intermediate valence state of cerium due to the strong hybridisation of 4f orbital of cerium with the localized π orbitals of conjugated phthalocyanine ligands, which differs from the situation for other analogues in the rare earth series that have the form $M^{III}(Pc^{2-})(Pc^{\bullet -})$. This actually is also true for the substituted bis(phthalocyaninato) and mixed (porphyrinato)[(na)phthalocyaninato] cerium complexes $Ce(Pc')_2$ [Pc′ = $Pc(OC_8H_{17})_8$, $Pc(t\text{Bu})_4$], Ce(TClPP)(Pc), and Ce(Por)(Nc) (Por = OEP, TBPP) [62]. The IR spectrum of $Ce(Pc^{2-})_2$ closely resembles those of the *reduced* double-deckers of tervalent rare earths $[NBu_4][M(Pc)_2]$ [73], which also demonstrates the dianionic nature of the phthalocyanine rings in $Ce(Pc)_2$. As shown in Fig. 2 and Table 1, significant differences exist in the pattern and characteristics of the IR spectrum of $Ce(Pc^{2-})_2$ compared with those of the tervalent rare earth bis(phthalocyaninato) counterparts. The marker IR band for phthalocyanine monoanion-radical, $Pc^{\bullet -}$, appearing at 1312–1323 cm^{-1} as the most or second most intense absorption band in the IR spectra of $M(Pc)_2$ (M = Y, La–Lu except for Ce and Pm) was not observed for $Ce(Pc)_2$. Instead, a significant peak appearing at 1329 cm^{-1} with medium intensity is assigned to the pyrrole stretching of the phthalocyanine dianion, Pc^{2-}. The most intense IR peak appears at 727 cm^{-1} due to the C–H wagging vibrations in the IR spectrum of $Ce(Pc)_2$, while the similar vibration shows the most or second most intense absorption around the same region for $M^{III}(Pc)_2$ (M = Y, La–Lu except for Ce and Pm) depending on the rare earth ionic size. Moreover, quite a strong absorption is observed at 1070 cm^{-1} attributed to the coupling of isoindole deformation and aza stretching in the IR spectrum of $Ce(Pc)_2$, which however is very weak in the spectra of tervalent rare earth phthalocyaninato double-decker analogues.

4.2. IR spectra of $M[Pc(OC_8H_{17})_8]_2$ and $M[Pc(tBu)_4]_2$ [9]

4.2.1. IR spectra of $M[Pc(OC_8H_{17})_8]_2$ [9]

Compared with those of $M(Pc)_2$, the IR spectra of the double-decker complexes $M[Pc(OC_8H_{17})_8]_2$ display several additional intense bands at about 1045, 1085, 1200, 1277, 1493–1500, 2854, 2869, 2925, and 2960 cm^{-1} [9]. However, the characteristic pattern of $M[Pc(OC_8H_{17})_8]_2$ IR spectra remains relatively simple, rather simpler than those of $M[Pc(t\text{Bu})_4]_2$, revealing the relatively higher symmetry of the former compounds. Comparison between the IR spectra of $Dy(Pc)_2$, $Dy[Pc(OC_8H_{17})_8]_2$, and $Dy[Pc(t\text{Bu})_4]_2$ having the same central metal, as shown in Fig. 3, together with knowledge of typical bands of alkyl groups, allows a clear identification of the IR vibrational fundamentals due to the octyloxy moieties (Table S1 (Supplementary data)). There are several important differences in the IR spectra between unsubstituted and octakis(octyloxy)-substituted bis(phthalocyaninato) rare earth complexes due to the octyloxy substituents. In the IR spectra of $M[Pc(OC_8H_{17})_8]_2$ (M = Y, La–Lu except for Ce and Pm) the IR marker band of phthalocyanine monoanion-radical $[Pc(OC_8H_{17})_8]^{\bullet -}$, in the region of 1311–1322 cm^{-1} loses some intensity to become a vibration with medium intensity, while the one at about 1375 cm^{-1} gains intensity to become a strong band. This contrasts with the observation of the most intense (or the second most intense) band at 1312–1323 cm^{-1} and a very weak peak at ca. 1370 cm^{-1} for $Pc^{\bullet -}$ in the IR spectra of $M(Pc)_2$ (M = Y, La–Lu except for Ce and Pm). This appears to suggest the octyloxy groups are responsible for apparently intensifying the weak isoindole stretching band of $M(Pc)_2$ at ca. 1370 cm^{-1} to a very strong absorption at ca. 1375 cm^{-1} for $M[Pc(OC_8H_{17})_8]_2$. Aroca and co-workers attributed the absorption at 1364 cm^{-1} with medium intensity to the C–H bending vibrations of *tert*-butyl groups in $Pr[Pc(t\text{Bu})_4]_2$ by comparing with the IR spectrum of $Pr(Pc)_2$ [27]. Indeed, it is well known that symmetric C–H deformations of the $–CH_3$ group usually give quite an intense absorption at ca. 1380 cm^{-1}. Therefore, the relatively intense band at ca. 1375 cm^{-1} for $M[Pc(OC_8H_{17})_8]_2$ is mainly contributed by the $–CH_3$ deformation due to the octyloxy side chains, together with some small contribution from the isoindole stretching vibrations.

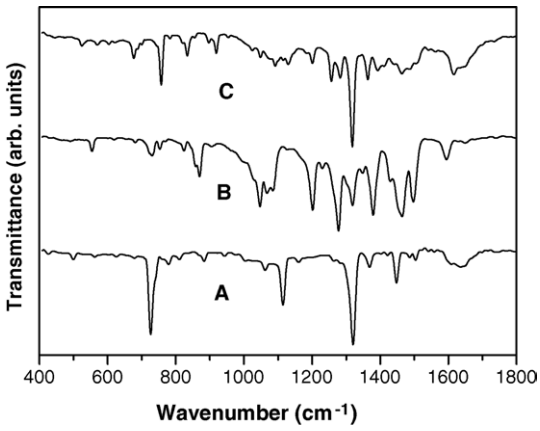

Fig. 3. IR spectra of (A) $Dy(Pc)_2$, (B) $Dy[Pc(OC_8H_{17})_8]_2$, and (C) $Dy[Pc(t\text{Bu})_4]_2$ in the region of 400–1800 cm^{-1} recorded in KBr pellets.

Furthermore, one of the most intense bands at around 725 cm^{-1} attributed to the aromatic C–H wagging vibrations in the spectra of $M(Pc)_2$, loses some intensity to become relatively weak in the spectra of $M[Pc(OC_8H_{17})_8]_2$. Substitution of H by OC_8H_{17} groups in all the peripheral β positions of Pc rings is considered to be responsible for decreasing the relative intensity of the out-of-plane C–H vibrations. The observation of the C–O–C stretching bands at ca. 1045 cm^{-1} (symmetric) and 1277 cm^{-1} (antisymmetric) seems to support this point. The relatively strong symmetric $–CH_2–$ bending and antisymmetric C–H deformations of $–CH_3$ groups of octyloxy side

chains, respectively, at about 1465 and 1460 cm^{-1} appear in a region in which only weak bands appear for unsubstituted bis(phthalocyaninato) rare earth compounds. It is still unclear at present why the weak peak attributed to the coupling of pyrrole and aza stretching at ca. 1500 cm^{-1} for $M(Pc)_2$ is replaced by quite an intense band in the IR spectra of $M[Pc(OC_8H_{17})_8]_2$. Finally, the most intense bands for the latter are the four absorptions at ca. 2854 cm^{-1} (CH_2 symmetric), 2870 cm^{-1} (CH_3 symmetric), 2925 cm^{-1} (CH_2 asymmetric), and 2955 cm^{-1} (CH_3 asymmetric) attributed to the C–H stretching vibrations of the octyloxy side chains.

The dianion nature of phthalocyanine in $Ce[Pc(OC_8H_{17})_8]_2$ is also revealed by its IR characteristics. The observation of an intense absorption at 1381 cm^{-1} together with a very weak band at ca. 1351 cm^{-1} constitute the characteristics of $[Pc(OC_8H_{17})_8]^{2-}$. In the IR spectrum of $Ce(Pc)_2$, the characteristic IR bands of phthalocyanine dianions in the region of 1300–1400 m^{-1} are an intense pyrrole stretching band at ca. 1330 cm^{-1} together with a very weak pyrrole and isoindole stretching coupling band at about 1370 cm^{-1}. This appears somewhat strange at first glance but can be easily understood on the basis of the characteristic IR bands of $Pc^{\bullet -}$ and $[Pc(OC_8H_{17})_8]^{\bullet -}$ in $M(Pc)_2$ and $M[Pc(OC_8H_{17})_8]_2$, respectively, in the same frequency range. The band at 1381 cm^{-1} is mainly attributed to the symmetric C–H deformation of $–CH_3$ groups with some contribution from the isoindole stretching vibrations.

In the IR spectra of $M[Pc(OC_8H_{17})_8]_2$, the vibrations at 1311–1322 cm^{-1} attributed to pyrrole stretching vibrations and at 1493–1500 cm^{-1} due to the coupling of the pyrrole stretching and aza stretching are sensitive to the ionic size of central rare earth ion. However, the other two rare earth size-dependent vibrations assigned to the coupling of isoindole breathing and C–H in-plane bending at 1110–1116 cm^{-1} and isoindole stretching at 1439–1454 cm^{-1} in the IR spectra of $M(Pc)_2$ could not be clearly delineated for $M[Pc(OC_8H_{17})_8]_2$ due to their overlap with neighbouring absorptions.

4.2.2. IR spectra of $M[Pc(tBu)_4]_2$ [9]

The IR spectra of the whole series of lanthanide compounds $M[Pc(tBu)_4]_2$ differ considerably from the simple patterns of the IR spectra of $M(Pc)_2$ and $M[Pc(OC_8H_{17})_8]_2$. The presence of four randomly-placed *tert*-butyl substituents on the phthalocyanine rings multiplies the number of IR active modes in $M[Pc(tBu)_4]_2$ due to the lower symmetry of most of the isomers. For the *tert*-butyl groups, three intense vibrations are seen in the C–H stretching region: $–CH_3$ antisymmetric stretching at 2957 and 2923 cm^{-1} and $–CH_3$ symmetric stretching at 2854 cm^{-1}. Absorptions with medium intensity observed in the range of 1358–1405 cm^{-1} are clearly mainly due to the symmetric $–CH_3$ deformation vibrations of *tert*-butyl groups together with some isoindole stretching, the latter exhibiting only very weak bands at about 1370 and 1400 cm^{-1} in the IR spectra of $M(Pc)_2$. The C–C stretching of the *tert*-butyl groups also displays quite a strong absorption at about 1255 cm^{-1}. The remaining bands in the region of 1000–1300 cm^{-1} are attributed to the aromatic in-plane C–H bending vibrations, including the medium intensity absorptions at 1091, 1200, and 1282 cm^{-1}. The relatively strong absorption at 752–758 cm^{-1} should be contributed from vibrations related to pyrrole or isoindole stretching, breathing or deformation or aza stretching vibrations of the Pc rings due to its rare earth size-dependent nature. As can be seen from Fig. 3, along with the change from unsubstituted or octakis(octyloxy)-substituted to tetra(*tert*-butyl)-substituted bis(phthalocyaninato) rare earth series, this absorption gains intensity to become a relatively strong band. This fact appears to suggest that the lower molecular symmetry of the isomers of $M[Pc(tBu)_4]_2$ is responsible for the observation of this peak. Aroca attributed the peak at 915 cm^{-1} in the IR spectrum of $Pr[Pc(tBu)_4]_2$ to the C–H bending of *tert*-butyl groups [27]. However, systematic research into the IR spectra of the whole series of $M[Pc(tBu)_4]_2$ complexes reveals that the frequency of this absorption with medium intensity at 914–919 cm^{-1} is dependent on the rare earth size, therefore this absorption should be better assigned as primarily originating from vibrations involving pyrrole or isoindole stretching, breathing or deformation or aza stretching vibrations of the Pc rings. The pyrrole ring stretching absorption at 1313–1319 cm^{-1} still appears as the most intense band as in the unsubstituted bis(phthalocyaninato) rare earth compounds. In contrast, the bands at ca. 725, 1115, and 1460 cm^{-1}, respectively, contributed from the C–H wagging, the coupling of isoindole breathing and C–H bending, and the isoindole stretching that are prominent in the spectra of the unsubstituted compounds appear as only weak or medium bands in the IR spectra of $M[Pc(tBu)_4]_2$.

Similar to $M(Pc)_2$ and $M[Pc(OC_8H_{17})_8]_2$, the vibrations at 752–758, 914–919, and 1313–1319 cm^{-1} in the IR spectra of $M[Pc(tBu)_4]_2$ shift slightly to higher energy along with the decrease of rare earth radius. The observation of an intense absorption at 1322 cm^{-1} in the IR spectrum of $Ce[Pc(tBu)_4]_2$, in contrast to the band at 1313–1319 cm^{-1} for tervalent rare earth analogues, is clear IR evidence of the dianion state of phthalocyanine in $Ce[Pc(tBu)_4]_2$.

One significant difference in the IR spectra between the two substituted bis(phthalocyaninato) rare earth series $M[Pc(OC_8H_{17})_8]_2$ and $M[Pc(tBu)_4]_2$ is the relative intensity of the C–H stretching vibrations with respect to the Pc ring stretching bands. In the IR spectra of $M[Pc(OC_8H_{17})_8]_2$, the most intense bands are C–H stretching modes of the octyloxy side chains. In the IR spectra of $M[Pc(tBu)_4]_2$, the most intense absorptions are the pyrrole stretching vibrations at 1313–1319 cm^{-1}, while the most intense absorption in the IR spectra of $M(Pc)_2$ is either the pyrrole stretching vibrations at 1312–1323 cm^{-1} or the C–H wagging band at ca. 725 cm^{-1} depending on identity of the rare earth metal ion.

4.3. IR spectra of $M[Pc(\alpha\text{-}OC_5H_{11})_4]_2$ [20]

Fig. 4 compares the IR spectra of $Yb(Pc)_2$, $Yb(Pc)[Pc(\alpha\text{-}OC_5H_{11})_4]$, and $Yb[Pc(\alpha\text{-}OC_5H_{11})_4]_2$, in the region of fundamental frequencies of 400–1800 cm^{-1}. The IR spectra of this new series of rare earth compounds $M[Pc(\alpha\text{-}OC_5H_{11})_4]_2$ differ considerably from the simple patterns of the IR spectra of $M(Pc)_2$. They very much resemble those of $M(Pc)[Pc(\alpha\text{-}OC_5H_{11})_4]$ except for the slight difference in the region

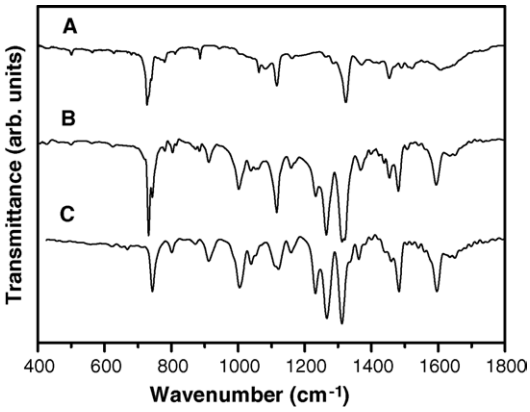

Fig. 4. IR spectra of (A) $Yb(Pc)_2$, (B) $Yb(Pc)[Pc(\alpha\text{-}OC_5H_{11})_4]$, and (C) $Yb[Pc(\alpha\text{-}OC_5H_{11})_4]_2$ in the region of 400–1800 cm^{-1} recorded in KBr pellets.

1110–1123 cm^{-1} attributed to the isoindole breathing coupled with C–H bending. In the IR spectra of both $M(Pc)_2$ and $M(Pc)[Pc(\alpha\text{-}OC_5H_{11})_4]$, there is a single band, but this splits into two absorption peaks at ca. 1110 and 1120–1123 cm^{-1} for $M[Pc(\alpha\text{-}OC_5H_{11})_4]_2$ [9,17]. Comparable spectroscopic features in the IR spectra between $M(Pc)[Pc(\alpha\text{-}OC_5H_{11})_4]$ and $M[Pc(\alpha\text{-}OC_5H_{11})_4]_2$ are not surprising considering the similar equilibrium geometry of the whole molecule, C_4 for $M(Pc)[Pc(\alpha\text{-}OC_5H_{11})_4]$ and S_8 for $M[Pc(\alpha\text{-}OC_5H_{11})_4]_2$, and in particular the same equilibrium geometry, C_4, for the fragment $M[Pc(\alpha\text{-}OC_5H_{11})_4]$ in both series of complexes.

The peak at ca. 743 cm^{-1} assigned to the C–H wagging gradually loses some intensity, relatively, in the order going from $M(Pc)_2$ (the most intense band), to $M(Pc)[Pc(\alpha\text{-}OC_5H_{11})_4]_2$ (one of the two most intense bands), and to $M[Pc(\alpha\text{-}OC_5H_{11})_4]_2$ (the fifth most intense band). This is due to the decrease in the number of aromatic H with increasing substitution by 3-pentyloxy groups in the non-peripheral α positions of the phthalocyanine rings.

The most interesting point concerns the frequency of the phthalocyanine monoanion radical IR marker band due to the pyrrole stretching in the range 1305–1313 cm^{-1}. When compared in Fig. 5, it is obvious that the frequency of the pyrrole stretching for bis(phthalocyaninato) complexes involving

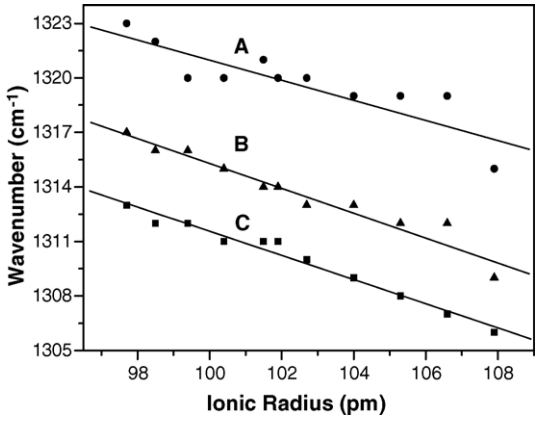

Fig. 5. Plot of wavenumbers of the pyrrole stretching vibrations of (A) $M(Pc)_2$, (B) $M(Pc)[Pc(\alpha\text{-}OC_5H_{11})_4]$, and (C) $M[Pc(\alpha\text{-}OC_5H_{11})_4]_2$ at 1306–1323 cm^{-1} as a function of the ionic radius of M^{III}.

the same rare earth ion is red-shifted in the order $M(Pc)_2$ to $M(Pc)[Pc(\alpha\text{-}OC_5H_{11})_4]$ to $M[Pc(\alpha\text{-}OC_5H_{11})_4]_2$, revealing the diminished ring-to-ring interaction in the same order [9,17]. However, a similar phenomenon was not found in comparing the IR spectroscopic characteristics of $M(Pc)_2$, $M(Pc)[Pc(OC_8H_{17})_8]$, and $M[Pc(OC_8H_{17})]_2$ [9,11]. This result indicates, from the viewpoint of vibrational spectroscopies, that substitution of alkoxyl groups at the non-peripheral α positions of phthalocyanine rings exerts more influence on the intrinsic properties of phthalocyanines than does peripheral β substitution.

4.4. IR spectra of $M(Pc)[Pc(OC_8H_{17})_8]$ [11]

Fig. S1 (Supplementary data) shows the IR spectra in the region 400–1800 cm^{-1} for three compounds $M(Pc)[Pc(OC_8H_{17})_8]$ (M = Nd, Dy, Yb), typical for the light, middle, and heavy rare earths, respectively. It is impossible to assign the observed frequencies to the individual unsubstituted and substituted phthalocyanine rings, due to the coupling of vibrational coordinates between the conjugated macrocycles.

As shown in Fig. S1 (Supplementary data), the IR spectra of the series of heteroleptic compounds $M(Pc)[Pc(OC_8H_{17})_8]$ differ considerably from the simple patterns of the IR spectra of $M(Pc)_2$, but resemble those of $M[Pc(OC_8H_{17})_8]_2$, except for the slightly increased complexity and number of vibration bands because of the reduced molecular symmetry. A comparison among the IR spectra of these three series confirms the identification of the IR vibrational fundamentals due to the phthalocyanine moieties and the peripheral octyloxy groups that was proposed previously by comparing the IR spectra of $M(Pc)_2$ and $M[Pc(OC_8H_{17})_8]_2$. This, in turn, makes it easier to assign the IR bands for these heteroleptic bis(phthalocyaninato) rare earth complexes. In the IR spectra of $M(Pc)[Pc(OC_8H_{17})_8]$, the pyrrole stretching at 1315–1322 cm^{-1} maintains its intensity as in $M(Pc)_2$, appearing as the most intense band, indeed more intense than in $M[Pc(OC_8H_{17})_8]_2$. It also acts as the phthalocyanine monoanion radical marker band. The C–H wagging of $M(Pc)[Pc(OC_8H_{17})_8]$ at ca. 725 cm^{-1} is less intense than that in $M(Pc)_2$, but reasonably is stronger than that in $M[Pc(OC_8H_{17})_8]_2$ due to the relative numbers of OC_8H_{17} groups in the peripheral β positions. In the IR spectra of $M(Pc)[Pc(OC_8H_{17})_8]$, the symmetric C–O–C stretching bands at 1045 cm^{-1}, the C–H band at 1203 cm^{-1}, the symmetric $-CH_3$ deformation at 1375 cm^{-1}, and the coupling of pyrrole and aza stretching at 1500 cm^{-1}, all lose some intensity relative to those in the IR spectra of $M[Pc(OC_8H_{17})_8]_2$. On the other hand, the antisymmetric C–O–C stretching band at 1275 cm^{-1} and the CH_2 bending at 1455 cm^{-1} have similar intensity to those in $M[Pc(OC_8H_{17})_8]_2$. Thus, in the region 400–1800 cm^{-1}, the antisymmetric vibrational bands of the octyloxy substituents maintain their intensity, whereas the symmetric vibrations, on the contrary, lose some intensity with the decrease of the number of octyloxy substituents.

Consistent with our results for other series, for $M(Pc)[Pc(OC_8H_{17})_8]$ the vibrations at 1057–1063 cm^{-1} due to the coupling of isoindole deformation and aza stretching, at

1315–1322 cm^{-1} attributed to pyrrole stretching vibrations, and at 1497–1504 cm^{-1} assigned to the coupling of pyrrole and aza stretching are sensitive to the ionic size of central rare earth ion.

4.5. IR spectra of M(Pc)[Pc(α-$OC_5H_{11})_4$] [17]

Fig. S2 (Supplementary data) shows typical IR spectra of three compounds M(Pc)[Pc(α-$OC_5H_{11})_4$] (M = Sm, Y, Yb). The IR spectra of this series of lanthanide compounds resemble those of M[Pc($OC_8H_{17})_8]_2$ and in particular M[Pc(α-$OC_5H_{11})_4]_2$ [20]. Compared with those of the former series and even M(Pc)[Pc($OC_8H_{17})_8$], the IR spectra of M(Pc)[Pc(α-$OC_5H_{11})_4$] display more fundamental absorptions due to the even lower molecular symmetry. Both isoindole breathing at 1112–1116 cm^{-1} and pyrrole stretching at 1309–1317 cm^{-1} maintain their intensity as in $M(Pc)_2$, appearing as the most intense bands. As for M(Pc)[Pc($OC_8H_{17})_8]_2$, the isoindole stretching of M(Pc)[Pc(α-$OC_5H_{11})_4$] shows weak peaks at ca. 1446–1457 cm^{-1} and the C–O–C stretching bands are observed as medium and strong bands at ca. 1040 cm^{-1} (symmetric) and 1265 cm^{-1} (antisymmetric), respectively.

Unlike in M[Pc($OC_8H_{17})_8]_2$ and M(Pc)[Pc($OC_8H_{17})_8$], with respect to the Pc ring stretching bands, the C–H stretching bands of the four 3-pentyloxy side chains are very weak due to the decrease in the length of the side chains from eight to five carbons.

In the IR spectra of M(Pc)[Pc(α-$OC_5H_{11})_4$], the vibrations at 1112–1116 cm^{-1} due to the isoindole breathing with some contribution from the C–H bending, 1309–1317 cm^{-1} attributed to pyrrole stretching vibrations and 1358–1372 cm^{-1} assigned to the coupling of pyrrole stretching vibrations and the symmetrical C–H deformation of $–CH_3$ groups are sensitive to the size of the central rare earth ion.

4.6. IR spectra of M[Nc(tBu)$_4]_2$ and M[Nc($SC_{12}H_{25})_8]_2$ [8]

4.6.1. IR spectra of M[Nc(tBu)$_4]_2$ [8]

Fig. 6 compares the IR spectra of four compounds M[Nc(*t*Bu)$_4]_2$ (M = Pr, Ce, Tb, Lu). The observed IR frequencies of the naphthalocyanine ligand are also partially assigned by analogy with their Raman characteristics [14], and the IR and Raman characteristics of bis(phthalocyaninato) rare earth counterparts [9,19], phthalocyanine [71] and naphthalocyanine derivatives [79–84].

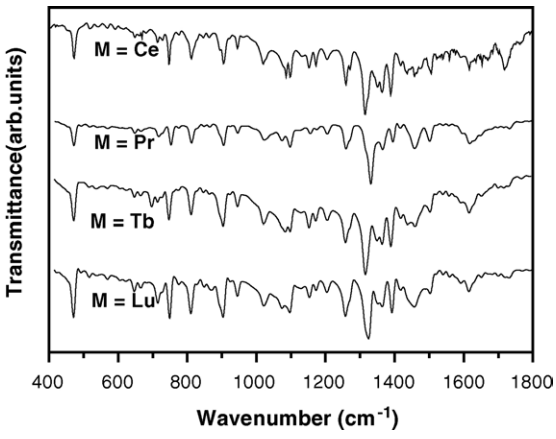

Fig. 6. IR spectra of M[Nc(*t*Bu$_4)_2$] (M = Ce, Pr, Tb, Lu) in the region of 400–1800 cm^{-1} recorded in KBr pellets.

The IR spectra of M[Nc(*t*Bu)$_4]_2$ differ considerably from the simple patterns of their Raman spectra [14] and from the IR spectra of the unsubstituted bis(phthalocyaninato) rare earth counterparts [9], but resemble the IR spectra of bis[tetra(*tert*-butyl)phthalocyaninato] rare earth compounds [9]. The complexity in the pattern of the IR spectra of M[Nc(*t*Bu)$_4]_2$ compared with that of M[Pc($OC_8H_{17})_8]_2$ [9] again reminds us of the lower molecular symmetry of the isomers that compose these mixtures. As for the *tert*-butyl substituted bis(phthalocyaninato) rare earth analogues M[Pc(*t*Bu)$_4]_2$ [9], characteristic vibrational fundamentals due to the Nc ring and the *tert*-butyl moieties were clearly identified. For the *tert*-butyl groups, three intense vibrations were seen for the C–H bond stretching vibrations at 2957 cm^{-1}, 2923 (antisymmetric stretching), and 2854 cm^{-1} (symmetric stretching). For the Nc ring, the C–H wagging at ca. 750, C–H bending at ca. 1080, and pyrrole ring stretching at 1315–1317 cm^{-1} still appear as intense bands as in the unsubstituted bis(phthalocyaninato) rare earth compounds. In contrast, the intense band at ca. 1460 cm^{-1} contributed from the isoindole stretching in $M(Pc)_2$ appears only as a weak or medium vibration in the IR spectra of M[Nc(*t*Bu)$_4]_2$. However, some weak vibrations in the IR spectra of unsubstituted bis(phthalocyaninato) rare earth compounds seem to gain additional intensity to become intense or medium intense bands in the IR spectra of M[Nc(*t*Bu)$_4]_2$. For instance, very intense absorptions were observed at 1260 (C–H bending of Nc ring), 1350–1355 (pyrrole stretching), and 1363–1367 cm^{-1} (naphthalene stretching) for M[Nc(*t*Bu)$_4]_2$, which exhibit only very weak bands at ca. 1282 and 1369 cm^{-1} in the IR spectra of $M(Pc)_2$ [9].

Confusion is evident in the literature regarding the specific nature of the vibrations of naphthalocyanine derivatives in the region of 1310–1370 cm^{-1}. Campos-Vallette et al. associated two bands at 1340–1350 and 1350–1370 cm^{-1} in the IR and Raman spectra of H_2Nc and Cu(Nc) with the pyrrole stretching and naphthalene stretching, respectively [82–84]. However, nothing was mentioned concerning the origin of the relatively strong vibrational peak in the region of 1310–1320 cm^{-1} (Raman) or 1320–1330 cm^{-1} (IR) for these two compounds. In comparing the IR spectroscopic characteristics with resolution of 2 cm^{-1} [8] and those with 4 cm^{-1} resolution [7], more vibrational modes have been resolved. This is typically revealed by comparing the vibrations of M[Nc(*t*Bu)$_4]_2$ in the region of 1310–1400 cm^{-1} (Fig. 6). Under the lower resolution IR conditions, four absorptions at ca. 1313–1331, 1350–1355, 1363–1367, and 1389–1394 cm^{-1}, whose frequencies all seem dependent on the rare earth metal, were observed in the region of 1300–1400 cm^{-1} [7]. With improved resolution of 2 cm^{-1}, the band at about 1313–1331 cm^{-1} is found to be composed of two vibrations of 1314–1317 and 1323–1330 cm^{-1}. Both the frequency and intensity of these two bands depend on the rare earth metal. Along with the rare earth contraction from La to

Lu, the intensity of the former absorption decreases while the latter one in contrast becomes more intense. In the IR spectra with lower resolution, this is the reason that the unresolved peak for the light rare earth bis(naphthalocyaninato) compounds is dominated by the absorption band at ca. 1313 cm^{-1} and the heavy rare earth bis(naphthalocyaninato) species by absorption at 1324–1331 cm^{-1} [7].

According to the previous work on the vibrational spectra of naphthalocyanine derivatives [30], it is reasonable to assign the absorptions at 1350–1355, 1363–1367, and 1389–1394 cm^{-1} to the pyrrole, naphthalene, and naphthalene stretching vibrations, respectively. Aroca and co-workers had attributed the absorption at 1364 cm^{-1} to the C–H bending vibrations of *tert*-butyl groups in Pr[Pc(*t*Bu)$_4$]$_2$ by comparing with the IR spectrum of Pc(Pc)$_2$ [27]. It is impossible to exclude absolutely the contribution from the *tert*-butyl groups on the naphthalocyanine rings in M[Nc(*t*Bu)$_4$]$_2$ to the weak absorption at ca. 1365 cm^{-1} in the present case. However, it may be concluded that the *major* contribution to this vibrational band is the naphthalene stretching mode based on the dependence of the frequency and the intensity of this peak on the rare earth size. Partly due to the same reason and by analogy to the assignment of the same absorptions in bis(phthalocyaninato) rare earth analogues, the two absorptions at 1314–1317 and 1323–1330 cm^{-1} for M[Nc(*t*Bu)$_4$]$_2$ are tentatively attributed to the pyrrole stretching vibrations of naphthalocyanine rings. The reason for the appearance of five relatively strong or strong absorption bands in the region from 1300 to 1400 cm^{-1} for M[Nc(*t*Bu)$_4$]$_2$ is not clear at this stage. The observation of only three absorptions in the same region for M[Nc($SC_{12}H_{25}$)$_8$]$_2$ also with high resolution of 2 cm^{-1} appears to suggest that it is due to the decreased symmetry of the M[Nc(*t*Bu)$_4$]$_2$ molecules.

The vibrations at 746–753 cm^{-1} assigned to the C–H wagging, 1314–1317, 1323–1330, and 1350–1355 cm^{-1} attributed to pyrrole stretching vibrations, and 1389–1394 cm^{-1} due to the naphthalene stretching vibrations shift slightly and linearly to higher energy along with the decrease of rare earth radius.

Among the whole series of tetra(*tert*-butyl)-substituted bis(naphthalocyaninato) rare earth complexes, the cerium double-decker is particularly interesting. As indicated from the electronic absorption, Raman, and ^{1}H NMR spectra, bis(naphthalocyaninato) cerium exists in the form Ce^{III}[Nc(*t*Bu)$_4^{2-}$][Nc(*t*Bu)$_4^{\bullet -}$], the same as other Nc analogues in the rare earth series [14,60,62]. It is clear that the IR characteristics of bis(naphthalocyaninato) cerium correspond well with all the other members of the series. As already noticed [8], the datum for Ce fits well with the trend observed between the ionic radius of M^{III} and the frequencies of the pyrrole stretching vibration near 1315 cm^{-1} for the whole series of double-decker compounds. This is a clear IR evidence proving the tervalent valence state of cerium in Ce[Nc(*t*Bu)$_4$]$_2$.

Similar to their phthalocyaninato analogues, the IR characteristics of naphthalocyanine dianion [Nc(*t*Bu)$_4$]$^{2-}$ could not be distinguished in the IR spectra of M[Nc(*t*Bu)$_4$]$_2$ and thus IR spectra of bis(naphthalocyaninato) rare earth(III) complexes can be attributed solely to the naphthalocyanine monoanion radical [Nc(*t*Bu)$_4$]$^{\bullet -}$. This demonstrates that the unpaired electron delocalizes over the two naphthalocyanine macrocycles on the IR vibration time scale, which accords well with the result deduced from the Raman spectra of the same compounds [14].

4.6.2. IR spectra of M[Pc($SC_{12}H_{25}$)$_8$]$_2$ [8]

The IR spectroscopic characteristics of bis[3,4,12,13,21,22,30,31-octa(dodecylthio)-2,3-naphthalocyaninato] rare earth complexes M[Nc($SC_{12}H_{25}$)$_8$]$_2$ are similar to those of their M[Nc(*t*Bu)$_4$]$_2$ analogues except for the simplicity due to the higher molecular symmetry of the former. Therefore, compared with those of M[Nc(*t*Bu)$_4$]$_2$, the IR spectra of M[Nc($SC_{12}H_{25}$)$_8$]$_2$ are composed of a relatively smaller number of fundamentals [9].

Another significant difference in the IR spectra between M[Nc(*t*Bu)$_4$]$_2$ and M[Nc($SC_{12}H_{25}$)$_8$]$_2$ is the relative intensity of the C–H stretching vibrations with respect to the stretching modes of the Nc rings. In the IR spectra of M[Nc($SC_{12}H_{25}$)$_8$]$_2$, the most intense bands are the absorptions at 2852, 2923, and 2986 cm^{-1} attributed to the C–H stretching vibrations of the eight dodecylthio groups. In contrast, in the IR spectra of M[Nc(*t*Bu)$_4$]$_2$, the most intense absorptions are those of the pyrrole stretching vibrations at ca. 1314–1317 or 1323–1330 cm^{-1} depending on rare earth species, and the C–H wagging at 758 cm^{-1}.

4.7. IR spectra of (Pc)M[Pc(OC_8H_{17})$_8$]M[Pc(OC_8H_{17})$_8$] [10]

Fig. 7 displays the IR spectrum of the representative compound (Pc)Er[Pc(OC_8H_{17})$_8$]Er[Pc(OC_8H_{17})$_8$]. Characteristic IR vibrational frequencies of the phthalocyanine ligand in this series are summarized and their interpretations are postulated by analogy with the IR characteristics of M(Pc′)$_2$ [Pc′ = Pc, Pc(OC_8H_{17})$_8$] [9]. Due to the similar molecular structure among the series of tris(phthalocyaninato) rare earth complexes, these compounds show similar IR characteristics, which can be reasonably understood on the basis of those of [M(Pc)$_2$]$^-$, and especially of Ce(Pc^{2-})$_2$ and Ce[Pc(OC_8H_{17})$_8^{2-}$]$_2$, due to the presence of phthalocyanine dianions in bis(phthalocyaninato) cerium compounds.

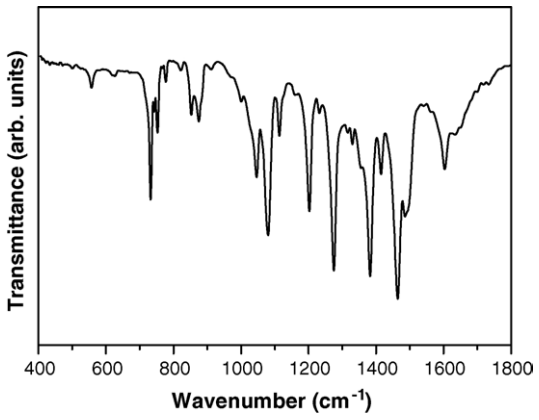

Fig. 7. IR spectrum of (Pc)Er[Pc(OC_8H_{17})$_8$]Er[Pc(OC_8H_{17})$_8$] in the region of 400–1800 cm^{-1} recorded in KBr pellets.

As shown in Fig. 7, the all-dianion nature of phthalocyanine ligands in (Pc)M[Pc(OC_8H_{17})$_8$]M[Pc(OC_8H_{17})$_8$] (M = Eu, Gd, Tb, Dy, Ho, Er, Yb, Lu, Y) is demonstrated by the following observations: (i) the absence of the very intense phthalocyanine monoanion-radical ($Pc'^{\bullet -}$) marker IR bands observed at 1312–1323 and 1311–1322 cm^{-1} respectively for $M^{III}(Pc)_2$ and M^{III}[Pc(OC_8H_{17})$_8$]$_2$; (ii) the appearance of quite a strong absorption at about 1380 cm^{-1}; and (iii) a relatively weak peak appearing at 1329 cm^{-1} together with a weak band at 1312–1317 cm^{-1}. These all correspond to the similar ones for tetravalent $Ce(Pc)_2$ and Ce[Pc(OC_8H_{17})$_8$]$_2$. The absorption at 1329 cm^{-1} for Pc^{2-} in $Ce(Pc)_2$ is a relatively strong peak, which loses some intensity to become a relatively weak absorption in the triple-deckers due to the ratio Pc:Pc(OC_8H_{17})$_8$ of 1:2 in these triple-decker compounds, while the intensity of the one at about 1380 cm^{-1} remains almost unchanged compared with that in double-decker Ce[Pc(OC_8H_{17})$_8$]$_2$. In addition, with the change of Pc:Pc(OC_8H_{17})$_8$ ratio from 1:2 in (Pc)M[Pc(OC_8H_{17})$_8$]M[Pc(OC_8H_{17})$_8$] to 2:1 in (Pc)Tm[Pc(OC_8H_{17})$_8$]Tm(Pc), there is no significant change in the intensity of the Pc^{2-} characteristic band at 1329 cm^{-1} and the Pc(OC_8H_{17})$_8{}^{2-}$ characteristic band at ca. 1380 cm^{-1}. For the weak band observed in the range of 1312–1317 cm^{-1} for (Pc)M[Pc(OC_8H_{17})$_8$]M[Pc(OC_8H_{17})$_8$], both Pc^{2-} and Pc(OC_8H_{17})$_8{}^{2-}$ are believed to contribute due to the observation of a similar weak absorption at 1306 and 1302 cm^{-1} respectively for $Ce(Pc)_2$ and Ce[Pc(OC_8H_{17})$_8$]$_2$. The appearance of two pyrrole stretching bands between 1300 and 1330 cm^{-1} for heteroleptic tris(phthalocyaninato) rare earth compounds is quite interesting, and is in line with the observation of two pyrrole stretching absorptions, respectively, at 1314–1317 and 1323–1330 cm^{-1} for M[Nc(*t*Bu)$_4$]$_2$. Another intense characteristic phthalocyanine dianion band appears at ca. 1080 cm^{-1} for (Pc)M[Pc(OC_8H_{17})$_8$]M[Pc(OC_8H_{17})$_8$]. This absorption corresponds to the similar one at ca. 1070 cm^{-1} in the IR spectrum of $Ce(Pc')_2$ [Pc′ = Pc, Pc(OC_8H_{17})$_8$] and is therefore similarly attributed to the coupling of isoindole deformation and aza stretching with some contribution also from C–H bending.

The relatively intense band at ca. 1380 cm^{-1} for (Pc)M[Pc(OC_8H_{17})$_8$]M[Pc(OC_8H_{17})$_8$] is assigned to C–H bendings of $–CH_3$ groups together with contribution from the isoindole stretching vibrations of the three phthalocyanine ligands. The contribution of the latter mode to this absorption is revealed by the dependence, although not very strong, of the energy of this band on the ionic size of rare earth metal. Moreover, the aromatic C–H wagging modes of Pc rings are responsible for one of the two most intense bands in the spectra of unsubstituted bis(phthalocyaninato) rare earth complexes $M(Pc)_2$ at around 725 cm^{-1}, that loses some intensity but remains relatively strong in the spectra of (Pc)M[Pc(OC_8H_{17})$_8$]M[Pc(OC_8H_{17})$_8$]. Substitution of H by OC_8H_{17} groups in all the peripheral β positions of two phthalocyanine rings in the molecule (Pc)M[Pc(OC_8H_{17})$_8$]M[Pc(OC_8H_{17})$_8$] is responsible for decreasing the relative intensity of the out-of-plane C–H vibrations. This observation is in line with the finding for M[Pc(OC_8H_{17})$_8$]$_2$ as further loss in intensity of this band was observed due to the complete β-substitution in these double-decker compounds [9].

Similar to Ce[Pc(OC_8H_{17})$_8$]$_2$ [9], the IR spectra of the triple-decker complexes (Pc)M[Pc(OC_8H_{17})$_8$]M[Pc(OC_8H_{17})$_8$] also display several additional intense fundamental bands at about 1047, 1080, 1203, 1275, 1494, 2854, 2870, 2924, and 2955 cm^{-1} in comparison with that for $Ce(Pc)_2$. A weak peak attributed to the coupling of pyrrole and aza stretching was observed at 1506 cm^{-1} for $Ce(Pc)_2$, while a relatively intense band appears at ca. 1495 cm^{-1} in the spectra of Ce[Pc(OC_8H_{17})$_8$]$_2$ [9]. In the present case, a band with medium intensity was found at ca. 1494 cm^{-1}. It is clear that the eight alkyloxy groups on the phthalocyanine ring are responsible for this vibrational mode. Further evidence derives from the fact that no enhancement was found for the same vibration in the homoleptic and heteroleptic analogues M^{III}[Pc(C_7H_{15})$_8$]$_2$ (M = Eu, Gd, Y), Ce[Pc(C_7H_{15})$_8$]$_2$, and M^{III}(Pc)[Pc(C_7H_{15})$_8$] [M = Eu, Y; H_2Pc(C_7H_{15})$_8$ = 2,3,9,10,16,17,24,25-octa(heptyl) phthalocyanine] [7].

In the IR spectra of (Pc)M[Pc(OC_8H_{17})$_8$]M[Pc(OC_8H_{17})$_8$], the weak vibration at 1312–1318 cm^{-1} attributed to pyrrole stretching vibrations shifts slightly to higher energy along with the decrease of rare earth radius, corresponding well with the observations for bis(phthalocyaninato) rare earth analogues [9,20] and clearly showing that the rare earth size effect also applies in the triple-deckers. The frequency of another pyrrole stretching vibration appears to remain almost unchanged at ca. 1329 cm^{-1}. This is strange, but is in line with the result obtained for a series of mixed ring rare earth triple-deckers M_2(TClPP)$_2$(Pc)$_2$ and M_2(TClPP)(Pc)$_2$ [H_2TClPP = 5,10,15,20-tetra(4-chlorophenyl)porphyrin], in which the characteristic Pc^{2-} IR band varies only from 1329 to 1331 cm^{-1} along with the lanthanide contraction from M = Pr to Ho [51]. Moreover, the wavenumbers of bands at 1381–1383 and 1463–1465 cm^{-1} mainly contributed by the C–H bending modes of octyloxy side chains seem also to show some small dependence on the rare earth ionic size, although not as significant as that for the pyrrole stretching band at 1312–1318 cm^{-1}. Therefore, these vibrations are reasonably assigned as being coupled with the isoindole stretching in the same region. The weaker dependence of corresponding vibrational frequencies, say the isoindole stretching at 1463–1465 cm^{-1} for tris(phthalocyaninato) compounds, on the rare earth ionic size, compared with that at 1439–1454 cm^{-1} for bis(phthalocyaninato) counterparts, shows that the π–π interactions in these heteroleptic triple-deckers are weaker than in double-deckers [9].

For the purpose of comparison, the IR spectrum of heterodinuclear analogue (Pc)Eu[Pc(OC_8H_{17})$_8$]Er[Pc(OC_8H_{17})$_8$] was also recorded. The frequency of the corresponding vibrational mode for this hetero-dinuclear rare earth complex (Pc)Eu[Pc(OC_8H_{17})$_8$]Er[Pc(OC_8H_{17})$_8$] at 1314 cm^{-1} lies just between those of the homo-dinuclear counterparts. This result is in line with that obtained from electrochemical studies of the same series of heteroleptic tris(phthalocyaninato) rare earth complexes, indicating again the strong delocalization between rings in the triple-decker complexes [85].

The IR spectrum of symmetrical di(phthalocyaninato)-mono[2,3,9,10,16,17,24,25-octakis(octyloxy)phthalocyaninato] rare earth triple-decker complex (Pc)Tm[Pc(OC_8H_{17})$_8$]Tm(Pc) was also recorded for comparison, and this actually resembles but appears simpler compared with those of less symmetrical analogues (Pc)M[Pc(OC_8H_{17})$_8$]M[Pc(OC_8H_{17})$_8$]. The difference in the Pc:Pc(OC_8H_{17})$_8$ ratios in these two species also results in changes in the relative intensities of corresponding vibrational modes. The presence of two unsubstituted Pc rings and only one substituted Pc(OC_8H_{17})$_8$ ligand in this compound naturally induces an increase in the intensity of characteristic bands attributed to Pc rings and decrease of those of the Pc(OC_8H_{17})$_8$ ring compared with those in (Pc)M[Pc(OC_8H_{17})$_8$]M[Pc(OC_8H_{17})$_8$]. The most obvious difference is the relative intensity of the C–H stretching vibrations with respect to the Pc ring stretching bands. In the IR spectra of the former series, the most intense band is the absorption at 2925 cm^{-1} due to the antisymmetric –CH_2– stretching vibrations of the octyloxy side chains of [Pc(OC_8H_{17})$_8$]. However, in the IR spectrum of the latter compound, the most intense absorption is a band at about 1465 cm^{-1} due to contribution from both C–H bending vibrations of the –CH_2– and –CH_3 groups and isoindole stretching vibrations.

5. Raman spectroscopic properties

5.1. Electronic absorption spectra

The appearance of the Raman spectra will be shown to depend on chemical composition, ionic radius of the coordinated metal ion, and the wavelength of excitation. Thus, it is important at the outset to appreciate the changes in electronic absorption spectra that govern the selective enhancement of certain Raman-active bands. The electronic absorption spectra of M(Pc)$_2$ and M[Pc(OC_8H_{17})$_8$]$_2$ (M = Pr, Tb, Tm) which are typical representatives of the UV–vis spectra for the complexes of tervalent rare earths in each series, are shown in Figs. 8 and 9, respectively [45]. All the spectra of M(Pc)$_2$ (M = Y, La–Lu except for Ce and Pm) show a typical B band at 316–325 nm with a very weak shoulder peak at the lower energy side of 342–358 nm

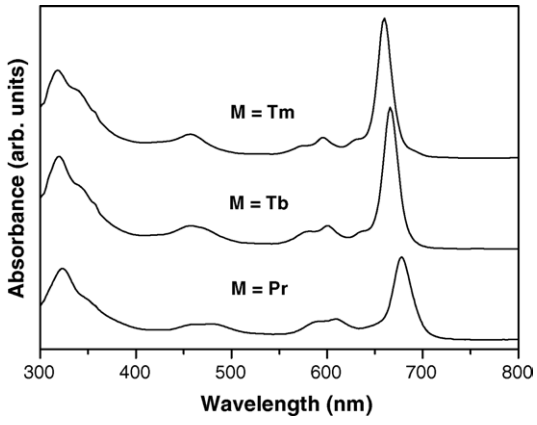

Fig. 8. The UV–vis spectra of M(Pc)$_2$ (M = Pr, Tb, Tm) in $CHCl_3$.

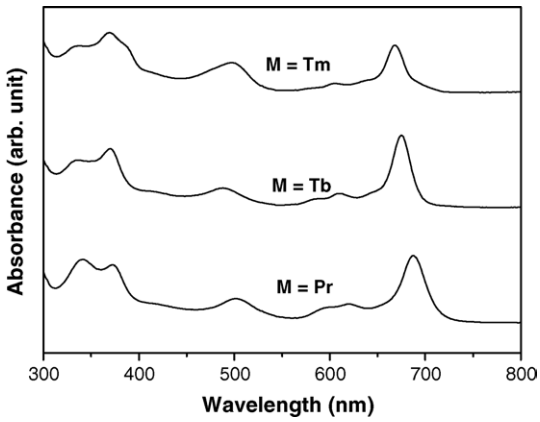

Fig. 9. The UV–vis spectra of M[Pc(OC_8H_{17})$_8$]$_2$ (M = Pr, Tb, Tm) in $CHCl_3$.

[86]. The Q bands for these compounds appear as a strong absorption in the range of 658–689 nm together with the weak vibronic components at 570–596 and 595–618 nm. In addition, a weak band related with the π-radical anion at 420–458 nm is also observed. For the series of M[Pc(OC_8H_{17})$_8$]$_2$ compounds containing tervalent rare earth metals, the B absorption splits into two bands at 331–343 and 369–378 nm due to the influence of eight octyloxy groups on the phthalocyaninato rings [45]. Their Q bands appear at 668–699 nm with weak vibronic absorptions at 579–601 and 604–630 nm, respectively. The weak π-radical anion band is seen at 485–513 nm. For both series of compounds, the energies of all the absorption bands mentioned above are sensitive to the metal center. In particular, along with the lanthanide contraction, the Q absorption band for both M(Pc)$_2$ and M[Pc(OC_8H_{17})$_8$]$_2$ blue-shifts in the same order [45,86]. These characteristics in their electronic absorption form the basis for the systematic changes that are observed in both the frequencies of specific bands and the overall appearances of the Raman spectra of M(Pc)$_2$ and M[Pc(OC_8H_{17})$_8$]$_2$ along with the change in the central metal ionic size, as detailed below. This is also true for other homoleptic and heteroleptic bis(phthalocyaninato) rare earth analogues M[Pc(α-OC_5H_{11})$_4$]$_2$ and M(Pc)[Pc(α-OC_5H_{11})$_4$] [53,54,69a], bis(naphthalocyaninato) rare earth compounds M[Mc(*t*Bu)$_4$]$_2$ [60,61], and even mixed (porphyrinato)(phthalocyaninato) rare earth double-decker compounds M(TClPP)(Pc) [50], and mixed (porphyrinato)(naphthalocyaninato) rare earth double-decker complexes M(Por)(Nc) (Por = OEP, TBPP) [55,56].

The electronic absorption spectra of M(TClPP)(Pc) (M = Ce, Sm, Ho), which are typical representatives of the UV–vis spectra for the intermediate-valent cerium (between III and IV) and light, middle, and heavy tervalent rare earth complexes, respectively, are shown in Fig. S3 (Supplementary data) [50]. In addition to the strong Pc and TClPP Soret bands respectively at 328–334 and 398–414 nm, the electronic absorption spectra of M(TClPP)(Pc) show a very weak Q band in the region of 689–738 nm for M = La–Lu, which is mainly contributed from the major Q absorption of the phthalocyanine monoanion radical by comparing with the absorption features of M(Pc)$_2$ [86]. This point actually is indirectly supported by the commonality of the features of the Raman spectra between M(TClPP)(Pc) and

$M(Pc)_2$ with excitation at either 633 or 785 nm [18]. This is also the case for M(Por)(Nc) (Por = OEP, TBPP) [15,16].

Except for $Ce[Nc(tBu)_4]_2$, which shows similar electronic absorption spectrum to the rest of the tervalent rare earth analogues, the other bis(tetrapyrrole) cerium complexes including Ce(TClPP)(Pc) (Fig. S3 (Supplementary data)), $Ce(Pc')_2$ [Pc′ = Pc, $Pc(OC_8H_{17})_8$, $Pc(tBu)_4$], and Ce(Por)(Nc) (Por = OEP, TBPP), display different electronic absorption spectra from their tervalent rare earth counterparts due to the valence state being intermediate between III and IV for the cerium in these double-decker compounds as suggested by the XANES results [62]. This is also reflected by the different IR and Raman spectroscopic characteristics of these cerium complexes from those of their tervalent rare earth counterparts [7–9,12,13,15,16,18,19].

5.2. Raman spectra of $M(Pc)_2$ and $M[Pc(OC_8H_{17})_8]_2$ [19]

5.2.1. Raman spectra of $M(Pc)_2$ and $M[Pc(OC_8H_{17})_8]_2$ with excitation by 633 nm laser [19]

The Raman spectra of $La(Pc)_2$ and $Dy[Pc(OC_8H_{17})_8]_2$ with excitation at 633 nm were of poor quality due to strong fluorescence. Figs. 10 and 11, respectively, compare the Raman spectra

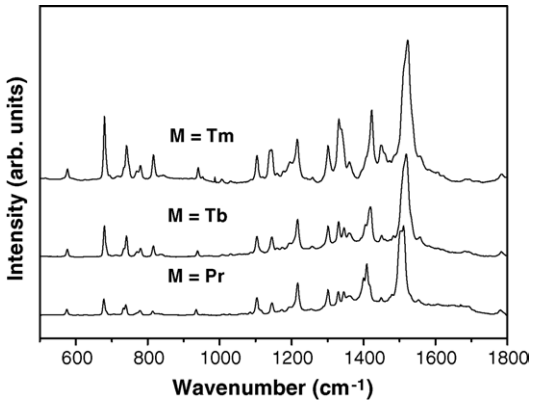

Fig. 10. Raman spectra of $M(Pc)_2$ (M = Pr, Tb, Tm) in the region of 500–1800 cm^{-1} with excitation at 633 nm recorded on a few grains of the solid sample.

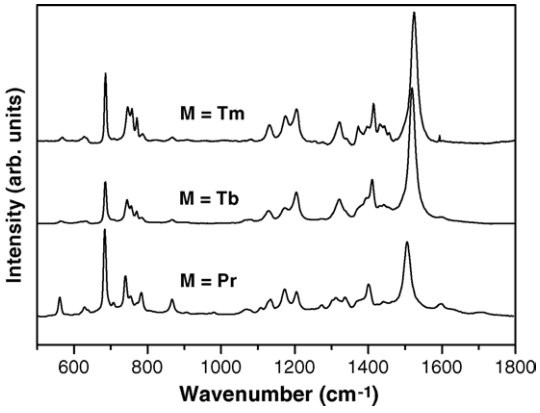

Fig. 11. Raman spectra of $M[Pc(OC_8H_{17})_8]_2$ (M = Pr, Tb, Tm) in the region of 500–1800 cm^{-1} with excitation at 633 nm recorded on a few grains of the solid sample.

of three compounds $M(Pc)_2$ and $M[Pc(OC_8H_{17})_8]_2$ for M = Pr, Tb, and Tm under excitation by 633 nm light. The Raman spectra for both series of compounds are fairly simple, revealing the high molecular symmetry of these compounds. In particular, the Raman spectra for the peripherally octa(octyloxy)-substituted bis(phthalocyaninato) rare earth complexes appear to be as simple as, or even simpler than, the corresponding unsubstituted counterparts $M(Pc)_2$, indicating that only frequencies corresponding to the characteristic fingerprint vibrations of the Pc macrocycle in $M[Pc(OC_8H_{17})_8]_2$ were observed. Side chain vibrations were very weak or absent under excitation with a laser line of 633 nm, and this is also true when using laser excitation at 785 nm. The observed Raman spectroscopic bands of phthalocyanine for these homoleptic bis(phthalocyaninato) complexes were partially assigned (Table 2) based on the previous description of normal modes for phthalocyaninato and especially bis(phthalocyaninato) metal derivatives [12–16,71]. Due to the similar electronic structure and electronic absorption properties among the whole series of bis(phthalocyaninato) rare earth compounds, all members of each series $M^{III}(Pc)_2$ and $M^{III}[Pc(OC_8H_{17})_8]_2$ (M = Y, La–Lu except Ce and Pm) show similar Raman characteristics.

With laser excitation at 633 nm, which is nearly in resonance with the Q band absorptions of both series of bis(phthalocyaninato) rare earth complexes, respectively, at 658–689 and 668–699 nm, Raman bands in the range of 1300–1600 cm^{-1} derived from isoindole ring stretching vibrations and the aza group stretching are selectively intensified. For $M^{III}(Pc)_2$, the weak bands at ca. 574–577 and 812–817 cm^{-1} and a band at 678–680 cm^{-1} with medium or strong intensity are attributed to phthalocyanine breathing [12,13,39–41], and the wavenumbers of all these modes show a dependence on the rare earth size, slightly blue-shifting along with the lanthanide contraction. The medium band at ca. 740 cm^{-1} is due to aromatic phthalocyanine C–H wagging [12,13]. In the range of 1000–1300 cm^{-1}, there are several weak or medium bands lying at ca. 1006, 1030, 1103, 1174, 1196, 1215, and 1301 cm^{-1}, which are assigned to aromatic C–H bending. The pyrrole breathing presents two bands in the region of around 1140 and 1500 cm^{-1}. The former comprises a single peak with medium intensity at ca. 1138–1145 cm^{-1} whereas the latter overlaps with the aza stretching vibration in the same region to form a broad band at 1495–1525 cm^{-1} for the whole series of compounds $M^{III}(Pc)_2$. For the double-deckers with early lanthanide metals, the aza stretching band appears as an unresolved shoulder on the *higher* energy side of the peak. In contrast, for the double-deckers with medium and late lanthanides, the pyrrole breathing band appears as an unresolved shoulder peak on the *lower* energy side of the more intense aza stretching peak. The intense band in the range 1409–1423 cm^{-1} and the weak band in the range 1444–1451 cm^{-1} are attributed to isoindole stretching vibrations. The former intense band discussed above, together with the aza stretching band at 1512–1525 cm^{-1} show dependence on the rare earth radius, also shifting to higher energy along with the rare earth contraction. This is not surprising considering the blue-shifted trend of the Q absorptions at 658–689 nm in the same order.

Table 2
Characteristic Raman bands (cm^{-1}) of phthalocyanines for $M[Pc(OC_8H_{17})]_2$ (M = Y, La–Lu except Pm and Dy) (λ_{ex} = 633 nm)

La	Ce	Pr	Nd	Sm	Eu	Gd	Tb	Y	Ho	Er	Tm	Yb	Lu	Assignment
561w	564w	562m	562w	562w	565w	564w	564w	568w	568w	568w	568w	568w	568w	Pc breathing
628w	625w	629w	629w	629w	634w	634w	632w	628w	629w	628w	628w	628w	636[a]	Pc breathing
683s	681s	684vs	684s	684s	684s	684s	686s	684s	684s	686s	686s	686s	686s	Pc breathing
741m	741m	741m	741m	742m	744m	744m	744w	745m	745w	745w	745w	747m	745m	C–H wag
753w	750w	755w	756w	755w	756w	756w	756w	757w	756w	756m	758m	758m	758m	
767w				771w	771w	771w	770w	771w	771w	771w	771w	771m	771w	C═N aza stretching
782w	780w	783w	783w	784w	783w	784w	784w	785w	785w	784w	787w	787w	787w	C═N aza stretching
866w	866w	867w	867w	867w	867w	867w	866w	866w	867w	867w	867w	867w	867w	Coupling of isoindole deformation and aza stretching C–H bend
1067w	1073w	1069w	1064w	1075w	1080w	1078w	1080w	1080w	1081w	1081w	1081w	1080w	1078w	
1135m	1135w	1135w	1135w	1132w	1130w	1130w	1128w	1130w	1132w	1130w	1132w	1132w	1132w	Pyrrole breathing
1174m	1173s	1173m	1173m	1173w	1173w	1173w	1173w	1174w	1174w	1174w	1174w	1174w	1176w	C–H bend
1205m	1199m	1205m	1205w	1205m	1205m	1205m	1205m	1205m	1205m	1205m	1205m	1205m	1205m	C–H bend
1316m	1299w	1312w	1312w	1319w	1321m	1321w	1321m	1321m	1321m	1321m	1322m	1322m	1322m	C═C pyrrole and benzene stretching
1335w	1350w	1336w	1339w	1338w										Isoindole stretching
								1371w	1371w	1371w	1373w	1373w	1373w	Isoindole stretching
1400m	1408m	1400m	1400m	1405s	1408s	1408s	1411s	1411s	1412s	1412s	1414m	1415s	1415m	Isoindole stretching
	1434m				1431w	1431w	1432w	1432w	1432w	1432w	1432w	1432w	1432w	Isoindole stretching
1444w	1461w	1440w	1443w	1441w	1440w	1441w	1440w	1442w		1443w	1443w	1445w	1444w	Isoindole stretching
								1457w	1457w	1457w	1457w	1457w	1457w	Isoindole stretching
1504vs	1501vs	1506s	1507vs	1513vs	1515vs	1516vs	1519vs	1521vs	1521vs	1522vs	1524vs	1525vs	1527vs	Coupling of pyrrole and aza stretching
1600w	1599w	1599w	1597w	1599w	1597w	1596w	1594w	1597w	1596w	1594w	1597w	1599w	1590w	Benzene stretching

[a] Shoulder band.

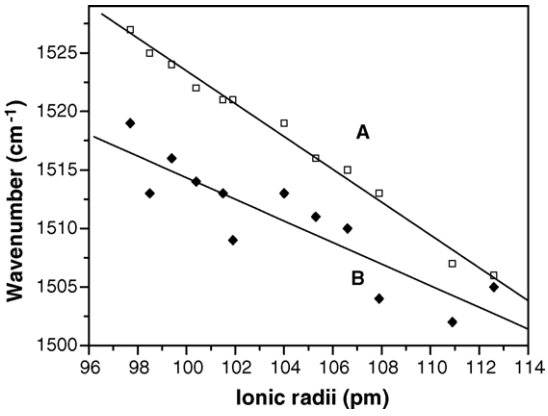

Fig. 12. Plot of wavenumber of the coupling of pyrrole and aza stretching scattering of (A) $M[Pc(OC_8H_{17})_8]_2$ and (B) $M(Pc)_2$ at 1504–1527 cm^{-1} with excitation at 633 nm as a function of the ionic radius of M^{III}.

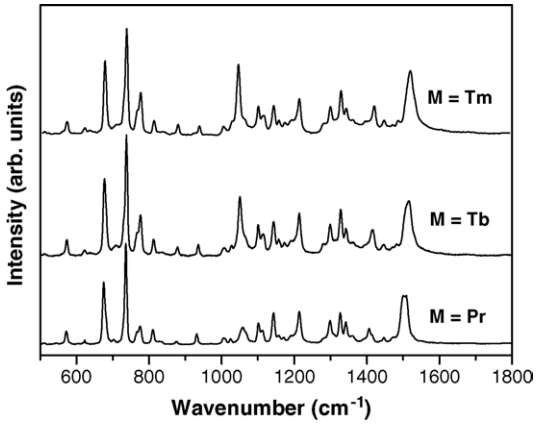

Fig. 13. Raman spectra of $M(Pc)_2$ (M = Pr, Tb, Tm) in the region of 500–1800 cm^{-1} with excitation at 785 nm recorded on a few grains of the solid sample.

As shown in Fig. 11, the Raman spectroscopic frequencies of the phthalocyanine core in $M[Pc(OC_8H_{17})_8]_2$ can be similarly assigned by analogy with those of unsubstituted counterparts $M(Pc)_2$. The spectra observed for $M[Pc(OC_8H_{17})_8]_2$ are even simpler than those of corresponding $M(Pc)_2$. This is probably due to the fact that the excitation at 633 nm is slightly further away from resonance with the main Q bands of $M[Pc(OC_8H_{17})_8]_2$ (668–699 nm) than with those of $M(Pc)_2$ and benefits the assignments of the frequencies. For instance, unlike for the series of $M^{III}(Pc)_2$, a very good linear correlation can be established between the frequency of the coupled pyrrole and aza stretching modes of $M^{III}[Pc(OC_8H_{17})_8]_2$ at 1504–1527 cm^{-1} and the tervalent rare earth ionic radii, as shown in Fig. 12. In addition, the band positions of the Pc breathing modes at 561–568 and 683–686 cm^{-1}, the C=N stretch at 782–787 cm^{-1}, the coupled C=C pyrrole and benzene stretching at 1312–1322 cm^{-1} and the isoindole stretching at 1400–1415 cm^{-1} show dependence on the rare earth ionic size. They all shift to higher energy along with the rare earth contraction as for their unsubstituted analogues.

The tervalent yttrium double-deckers are noteworthy. The wavenumbers of some above-mentioned bands for both $Y^{III}(Pc)_2$ and $Y^{III}[Pc(OC_8H_{17})_8]_2$ deviate from the linear relationship established for the other tervalent rare earth complexes (for example, see Table 2), due probably to the intrinsic difference between yttrium and the lanthanides, namely the absence of f electrons. This is also true for these two yttrium complexes when using laser excitation emitting at 785 nm.

As can be expected from the previous studies [12,13,18], both $Ce(Pc)_2$ and $Ce[Pc(OC_8H_{17})_8]_2$ show different Raman spectroscopic characteristics from those of the rest of the rare earth series, which is related to the different electronic absorption spectra of these cerium complexes. As indicated above, both phthalocyanine rings exist as dianions in $Ce(Pc)_2$ and $Ce[Pc(OC_8H_{17})_8]_2$, despite the valence state intermediate between III and IV for the cerium [62]. These complexes therefore differ from other analogues that have the form $M(Pc'^{2-})(Pc'^{\bullet -})$ [Pc′ = Pc, $Pc(OC_8H_{17})_8$]. A comparison of the Raman spectra of $Ce(Pc)_2$ and $Ce[Pc(OC_8H_{17})_8]_2$ with those of the rest of the series shows that these cerium complexes contain most of the bands found for the other complexes, however the relative intensities are different. For example, a strong band appears at 1173 cm^{-1} for $Ce[Pc(OC_8H_{17})_8]_2$ (Table 2) corresponding to C–H bending, but for the other complexes, only a weak band in the same region is observed. Moreover, the marker Raman band of Pc^{2-} and $[Pc(OC_8H_{17})_8]^{2-}$ at 1499 and 1501 cm^{-1}, respectively, with contributions from pyrrole C=C, aza C=N and isoindole stretches, is observed as the strongest scattering in the Raman spectra of $Ce(Pc)_2$ and $Ce[Pc(OC_8H_{17})_8]_2$. As noted above, a similar strong band due to $Pc^{\bullet -}$ and $[Pc(OC_8H_{17})_8]^{\bullet -}$ has been found to upshift to 1502–1509 and 1504–1527 cm^{-1} in the Raman spectra of $M^{III}(Pc)_2$ and $M^{III}[Pc(OC_8H_{17})_8]_2$.

5.2.2. Raman spectra of $M(Pc)_2$ and $M[Pc(OC_8H_{17})_8]_2$ with excitation by 785 nm laser [19]

Strong fluorescence occurred when trying to record the Raman spectra of $M(Pc)_2$ (M = La, Ce, Lu) using excitation at 785 nm, so these data do not appear. Using the excitation laser line at 785 nm that is far away from resonance with the Q absorption bands, as shown in Fig. 13, the macrocyclic ring deformation and ring radial vibrations between 500 and 1000 cm^{-1} in the Raman spectra of $M(Pc)_2$ are selectively intensified. This is in good accordance with the result of Ostendorp and Homborg [36]. The Pc breathing at 675–679 cm^{-1} and the aromatic C–H wagging at ca. 739 cm^{-1} are the most intense bands. The band locating at 1327–1329 cm^{-1} with medium intensity is assigned to the pyrrole C=C stretching vibrations coupled with benzene C=C stretching vibrations and the weak one at about 1342 cm^{-1} to the isoindole stretching vibrations. Similar to those excited with 633 nm laser line, the bands of the coupled pyrrole C=C and aza C=N stretching vibrations in the region of 1507–1521 cm^{-1} overlap to form a broad, unresolved envelope. The vibrations of $M(Pc)_2$ at 675–679 cm^{-1} assigned to the Pc breathings, at 1407–1422 cm^{-1} attributed to the isoindole stretching vibrations, and at 1508–1521 cm^{-1} due to the coupling of aza and pyrrole stretching vibrations are found to shift to higher energy along with the ionic radius contraction.

Under the same laser line excitation of 785 nm, the Raman spectra for the octa(octyloxy)-substituted bis(phthalocyaninato)

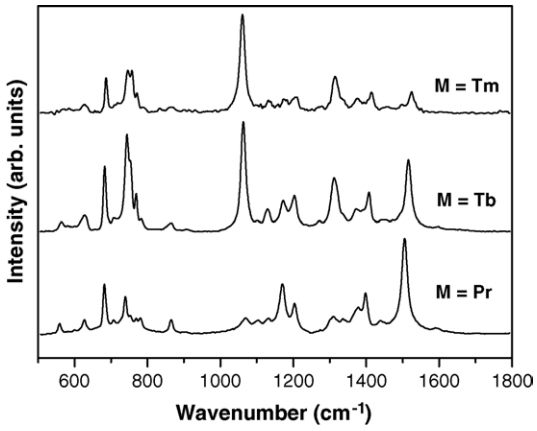

Fig. 14. Raman spectra of M[Pc(OC_8H_{17})$_8$]$_2$ (M = Pr, Tb, Tm) in the region of 500–1800 cm^{-1} with excitation at 785 nm recorded on a few grains of the solid sample.

rare earth analogues M[Pc(OC_8H_{17})$_8$]$_2$ basically exhibit the same spectroscopic features as corresponding unsubstituted counterparts M(Pc)$_2$ (Table S2 (Supplementary data)). However, this time a systematic but rather more dramatic change can be seen in the appearance of the Raman spectra across the series. Along with the decrease in the ionic size from La to Lu, the band at 1502–1528 cm^{-1} contributed from the coupling of the pyrrole and aza stretching vibrations gradually loses some intensity, changing from a very strong scattering for the light rare earth compounds to a medium and weak one for the heavy rare earth complexes. In the same order, the band at ca. 1060 cm^{-1} assigned to the C–H bendings in contrast gradually gains intensity to change from a weak band to an intense band. A similar change in the intensity of the latter band at ca. 1050 cm^{-1} due to the C–H bending was also observed in the Raman spectra of M^{III}(Pc)$_2$ under the same laser line excitation. However, the change in the intensity of the former band for M^{III}(Pc)$_2$ was not so significant. All these results can be clearly exemplified by the Raman spectra of the Pr, Tb, and Tm complexes of the two series shown in Figs. 13 and 14.

When exciting the Raman spectrum of Ce[Pc(OC_8H_{17})$_8$]$_2$ with the 785 nm laser line, similar to the case using the 633 nm laser line, a Raman spectrum with different characteristics from those of the rest of the rare earth series was obtained. The intense band at 1498 cm^{-1} with contribution from both pyrrole C=C and aza C=N stretches together with isoindole stretching vibrations is the marker Raman band of [Pc(OC_8H_{17})$_8$]$^{2-}$, which compares with that of [Pc(OC_8H_{17})$_8$]$^{\bullet -}$ at 1502–1528 cm^{-1} in the Raman spectra of M^{III}[Pc(OC_8H_{17})$_8$]$_2$ under the same excitation.

5.3. Raman spectra of M[Pc(α-OC_5H_{11})$_4$]$_2$ [20]

Since the Raman spectra of M[Pc(α-OC_5H_{11})$_4$]$_2$ recorded with excitation at 785 nm were of poor quality, the Raman scattering of M[Pc(α-OC_5H_{11})$_4$]$_2$ was described only for laser excitation at 633 nm and their interpretations are proposed by analogy with the vibrational characteristics of bis(phthalocyaninato) metal derivatives, in particular M(Pc)$_2$ and M(Pc)[Pc(α-OC_5H_{11})$_4$] [9,17,19].

Fig. S4 (Supplementary data) compares the Raman spectra of three compounds M[Pc(α-OC_5H_{11})$_4$]$_2$ for M = Eu, Y, and Lu under excitation by 633 nm light. As for the IR spectra, the Raman spectra for M[Pc(α-OC_5H_{11})$_4$]$_2$ appear relatively more complicated than those of the homoleptic analogues M(Pc)$_2$ and M[Pc(OC_8H_{17})$_8$]$_2$. In addition, unlike the IR spectra, the Raman spectra of M[Pc(α-OC_5H_{11})$_4$]$_2$ show different characteristic appearances from those of M(Pc)[Pc(α-OC_5H_{11})$_4$]$_2$ under the same laser line excitation, due to the difference in the Q absorption between the two series of complexes [17]. Because of the similar electronic structure among the whole series of bis(phthalocyaninato) rare earth compounds and the gradual and systematic change in the Q absorptions of the same series [69a], M[Pc(α-OC_5H_{11})$_4$]$_2$ (M = Y, Pr–Lu except for Pm) show similar spectroscopic characteristics with gradual change in their Raman appearance. Along with the decrease in the ionic size from Pr to Lu, the resolution in the Raman spectrum of double-decker compounds gradually increases (Fig. S4 (Supplementary data)) [20]. This result is contrary to that for the Raman spectra of M(Pc)[Pc(α-OC_5H_{11})$_4$] [17].

With laser excitation at 633 nm, which is nearly coincident with two of the three or four Q band absorptions of bis(phthalocyaninato) rare earth complexes in the range of 634–716 nm, vibrational bands in the range of 1300–1600 cm^{-1} derived from isoindole ring stretching vibrations and the aza group stretching are selectively intensified as expected. In the range of 1000–1300 cm^{-1}, there are several medium and strong bands lying at 1109, 1161, 1177, 1239, and 1306 cm^{-1}, which are assigned to aromatic C–H bending. The wavenumbers of this scattering are almost constant for the whole series of compounds. The pyrrole breathing presents two bands in the region close to 1138 and 1495 cm^{-1}. The former one remains as a single peak with weak or medium intensity at ca. 1126–1140 cm^{-1}, whereas the latter one overlaps with the aza stretching in the same region. For M[Pc(α-OC_5H_{11})$_4$]$_2$ when M = Pr and Nd, a broad band at 1500–1506 cm^{-1} is observed in which the aza stretching band in the *higher* energy side appears as unresolved shoulder peak. For the double-deckers M[Pc(α-OC_5H_{11})$_4$]$_2$ with M = Sm to Gd, a broad scattering at 1521–1524 cm^{-1} can be seen in which the pyrrole breathing band appears as an unresolved shoulder in the *lower* energy side. Along with the further decrease in the central rare earth ionic size from Tb to Lu, two well-separated peaks at ca.1495–1500 and 1526–1530 cm^{-1}, respectively, contributed mainly from the pyrrole breathing and aza stretching, were observed in their Raman spectra. It is noteworthy that the wavenumbers of the aza stretching band together with the bands at 1393–1405 and 1409–1426 cm^{-1} due to isoindole stretching vibrations show dependence on the rare earth radius.

5.4. Raman spectra of M(Pc)[Pc(α-OC_5H_{11})$_4$] [17]

5.4.1. Raman spectra of M(Pc)[Pc(α-OC_5H_{11})$_4$] with excitation by 633 nm laser [17]

Characteristic Raman vibrational bands of the phthalocyanine ligand in M(Pc)[Pc(α-OC_5H_{11})$_4$] (M = Y, Sm–Lu) have been recorded under excitation by both laser lines, namely 633 and 785 nm. Fig. S5 (Supplementary data) compares the

Raman spectra of three compounds M(Pc)[Pc(α-$OC_5H_{11})_4$] for M = Sm, Dy and Lu under excitation by 633 nm light. The spectra for M(Pc)[Pc(α-$OC_5H_{11})_4$] seem to be relatively complicated compared with those of $M(Pc)_2$ and M[Pc($OC_8H_{17})_8]_2$ [19] due to their relatively lower symmetry. By analogy with their homoleptic bis(phthalocyaninato) rare earth counterparts [12,13,19], interpretations of vibrational characteristics for these heteroleptic complexes have been proposed [17].

Similar to the case of M[Pc(α-$OC_5H_{11})_4]_2$, with laser excitation at 633 nm, which is nearly coincident with two of the three Q band absorptions of bis(phthalocyaninato) rare earth complexes at 616–630 and 645–662 nm, peaks in the range of 1300–1600 cm^{-1} are selectively intensified. In the range of 1000–1300 cm^{-1}, several weak or medium bands lying at 1103, 1161, 1175, 1193, 1214, and 1300 cm^{-1}, whose wavenumbers are almost constant for the whole series of compounds, are attributed to the aromatic C–H bending. Noteworthy again is the pyrrole breathing band at ca.1500 cm^{-1}, which overlaps with the aza stretching vibration in the same region to form a broad band at 1499–1502 cm^{-1} for M(Pc)[Pc(α-$OC_5H_{11})_4$] from M = Sm to Tb, in which the aza stretching band in the higher energy side appears as unresolved shoulder peak. For the double-deckers M(Pc)[Pc(α-$OC_5H_{11})_4$] with M = Dy to Er including Y, two well-separated bands at 1506–1509 and 1513–1515 cm^{-1} contributed mainly from the pyrrole and aza stretching vibrations, respectively, were observed. Further decrease in the central rare earth ionic size again induces the coalescence of these two vibrations, i.e. the C=C pyrrole and C=N aza stretching vibrations. This time, the aza stretching seems to dominate the overlapped scattering, showing a broad band centered at 1525–1528 cm^{-1} for M(Pc)[Pc(α-$OC_5H_{11})_4$] (M = Tm, Yb, Lu), and the weak pyrrole stretching vibration is covered in the lower energy side of this broad scattering. Two bands at 1417–1425 and 1445–1451 cm^{-1} are observed due to isoindole stretching vibrations. All the three bands discussed above show dependence on the rare earth radius. Actually, a systematic change could also be seen in the overall appearance of the Raman spectra of M(Pc)[Pc(α-$OC_5H_{11})_4$]. Along with the decrease in the ionic size from Sm to Lu, the resolution in the Raman spectrum of double-decker compounds gradually decreases (Fig. S5 (Supplementary data)). This trend is just in contrast to that observed for the Raman spectra excited with 785 nm laser line as shown in Fig. S6 (Supplementary data), and to that observed for the homoleptic counterparts M[Pc(α-$OC_5H_{11})_4]_2$ when excited with the 633 nm laser line [20].

5.4.2. *Raman spectra of M(Pc)[Pc(α-$OC_5H_{11})_4$] with excitation by 785 nm laser [17]*

Using excitation at 785 nm whose wavelength is far away from resonance with the Q absorption bands of M(Pc)[Pc(α-$OC_5H_{11})_4$], as shown in Fig. S6 (Supplementary data), the macrocyclic ring deformation and ring radial vibrations between 500 and 1000 cm^{-1} are selectively intensified. This is in good accordance with the Raman characteristics of homoleptic bis(phthalocyaninato) rare earth analogues [19,36]. The Pc breathing at 676–681 cm^{-1} and the aromatic C–H wagging at ca. 745 cm^{-1} are the most intense bands. Similar to those excited with 633 nm laser line, the frequencies of the coupling of pyrrole C=C and aza C=N stretching vibrations at 1510 cm^{-1} and the aza stretching in the region around 1520 cm^{-1} overlap to form a broad band, which is further covered with another intense aza stretching vibration at 1523–1538 cm^{-1} and therefore appears as a broad, unresolved envelope in the range of 1509–1522 cm^{-1}.

Under 785 nm excitation, the vibrations at 676–681 cm^{-1} assigned to the Pc breathings, at 1420–1428 and 1448–1455 cm^{-1} attributed to the isoindole stretching vibrations, and at 1509–1522 and 1523–1538 cm^{-1} due to the coupling of aza and pyrrole stretching vibrations are found to shift to higher energy along with the ionic radius contraction.

5.5. *Raman spectra of M[Nc(tBu)$_4$]$_2$ [14]*

5.5.1. *Raman spectra of M[Nc(tBu)$_4$]$_2$ with excitation by 633 nm laser [14]*

Fig. 15 compares the Raman spectra obtained with excitation at 633 nm of three compounds M[Nc(*t*Bu)$_4]_2$ (M = Ce, Gd, Lu), typical for the light, middle, and heavy rare earths, respectively. The observed Raman bands of naphthalocyanine for M[Nc(*t*Bu)$_4]_2$ were also partially assigned by analogy with the Raman characteristics of bis(phthalocyaninato) rare earth counterparts [12,13,19] and naphthalocyanine derivatives [79–84]. The naphthalene stretching vibrations around 1592 cm^{-1} appear as the most intense band. The Nc breathing mode in M[Nc(*t*Bu)$_4]_2$ appears as a weak band at ca. 681–684 cm^{-1}, which gains intensity gradually from M = Ce to Lu and shows a trend to blue-shift slightly along with the decrease of rare earth radius. The pyrrole stretching gives two peaks at ca. 1154 and 1500 cm^{-1}. The former one remains unchanged at ca. 1154 cm^{-1} as a single weak peak whereas the latter one seems to be blue-shifted along with the rare earth contraction. This latter peak overlaps with the aza stretching vibration at ca. 1520 cm^{-1} and thus appears as a shoulder for M[Nc(*t*Bu)$_4]_2$ from M = Ce to Tm. Only in the spectra of the smallest rare earth bis(naphthalocyaninato) compounds M[Nc(*t*Bu)$_4]_2$ (M = Yb, Lu) is this vibration apparent as a well-separated band at 1512 and 1513 cm^{-1}, respectively. The sensitivity of this vibrational mode to the central metal radius in

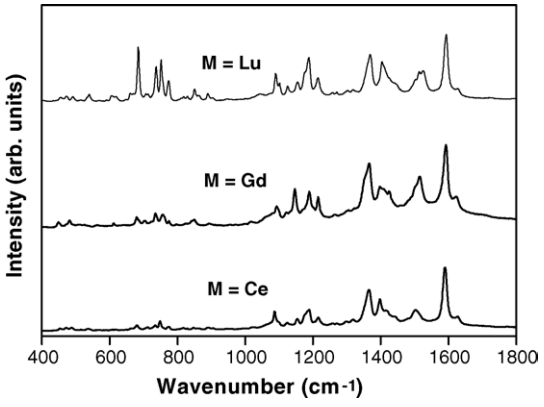

Fig. 15. Raman spectra of M[Nc(*t*Bu)$_4]_2$ (M = Ce, Gd, Lu) with excitation at 633 nm recorded on a few grains of the solid sample.

the complexes suggests that it must contain significant C=N aza character and therefore is assigned to the coupling of pyrrole C=C and aza C=N stretches, which is consistent with the point of Melendres on the same vibrational mode of phthalocyanine derivatives [87]. The weak bands in the region from 400 to 1000 cm^{-1} are assigned to the ring radial vibrations of the isoindole moieties and the naphthalocyanine macrocycle. One of these at 750 cm^{-1} is due to the aromatic naphthalocyanine C–H wagging, which also gains intensity along with the decrease of rare earth size from Ce to Lu just as does that at 684 cm^{-1} due to the Nc ring breathing.

The bands with weak and medium intensity observed in the 1050–1280 cm^{-1} region are attributed to the in-plane naphthalocyanine C–H bending vibrations. The remaining vibrations in the range of 1320–1650 cm^{-1} are isoindole, aza group, and naphthalene stretches. In this group, except for the above-mentioned band at 1503–1513 cm^{-1} derived from the coupling of pyrrole C=C and aza C=N stretches, the C=N aza group stretch exhibits a weak shoulder band at ca. 1515 cm^{-1} for Ce[Nc(tBu)$_4$]$_2$ and a weak separated band at 1524 cm^{-1} for Lu[Nc(tBu)$_4$]$_2$. The most intense vibration at ca. 1592 cm^{-1} and a very weak shoulder at ca. 1625 cm^{-1} are assigned to the naphthalene stretches in M[Nc(tBu)$_4$]$_2$ (M = Y, Ce–Lu except Nd and Pm) by analogy with those of bis(phthalocyaninato) rare earths and monomeric naphthalocyaninato-metal compounds [12,13,19,21]. In our preliminary and previous report on the Raman spectra of several double-deckers M[Nc(tBu)$_4$]$_2$, we tentatively assigned the intense band at ca. 1370 cm^{-1} to the pyrrole vibration [12]. However, according to its appearance with a shoulder at ca. 1340 cm^{-1} and the sensitivity of this wavenumber to the nature of the rare earth ion, we now revise our assignment of the broad band centred at 1364–1369 cm^{-1}, and attribute it to the overlapped vibrations of the naphthalene stretching with some contributions from the pyrrole stretching vibrations. This has been verified by the corresponding characteristics of the same band in M(OEP)(Nc) [15].

Under excitation at 633 nm, the vibrations at 681–684 cm^{-1} assigned to the Nc breathing, 1357–1361 cm^{-1} due to the naphthalene stretching vibrations, 1409–1415 cm^{-1} attributed to the isoindole stretching vibrations, and 1517–1530 cm^{-1} contributed from the aza stretching vibrations in the Raman spectra of M[Nc(tBu)$_4$]$_2$ shift slightly to higher energy along with the decrease of rare earth radius. A vibration in the range of 849–854 cm^{-1} seems also to show such a trend, shifting slightly from 849 cm^{-1} for Ce[Nc(tBu)$_4$]$_2$ to 853 cm^{-1} for Lu[Nc(tBu)$_4$]$_2$. It seems that the present results support Shurvell and Pinzuti [71] and Janczak [88] who associated the band in the range of 810–830 cm^{-1} with the metal–ligand vibration. Anyway, more theoretical and experimental efforts are necessary to make clear assignment of the frequencies in the region from 800 to 900 cm^{-1} to the metal–nitrogen vibration.

5.5.2. *Raman spectra of M[Nc(tBu)$_4$]$_2$ with excitation by 785 nm laser [14]*

Using excitation at 785 nm, as shown in Fig. 16, the macrocyclic ring deformation and ring radial vibrations between 400 and 900 cm^{-1} in the Raman spectra of M[Nc(tBu)$_4$]$_2$ are selectively intensified. This is in good accordance with the Raman characteristics of bis(phthalocyaninato) rare earth analogues [19]. The Nc breathing at ca. 682 cm^{-1} and the aromatic C–H wagging at ca. 738 cm^{-1} are the most intense bands. The intense band due to the naphthalene stretches around 1592 cm^{-1} under 633 nm excitation is absent, whereas the vibration at ca. 1637 cm^{-1} remains as a very weak band. Similar to those excited with 633 nm laser line, the wavenumbers of the coupling of pyrrole C=C and aza C=N stretches at 1508 cm^{-1} and the aza stretch in the region above 1520 cm^{-1} overlap to form a broad band. For the bis(naphthalocyaninato) complexes of larger rare earths such as Ce and Pr, the contribution from coupling of pyrrole C=C and aza C=N stretches dominates and the two overlapped vibrations show a broad weak band at 1508 and 1507 cm^{-1}, respectively. For metals heavier than Sm, the appearance of the two overlapped vibrations is dominated by the contribution of the aza stretches and a relatively intense and broad band shifts from 1512 cm^{-1} for Sm[Nc(tBu)$_4$]$_2$ to 1524 cm^{-1} for Lu[Nc(tBu)$_4$]$_2$. Obviously, the application of the 785 nm laser line makes the intensity of this vibration stronger than using the 633 nm laser line and its frequency is clearly also dependent on the size of the metal ion. The broad, weak band locating at 1357–1361 cm^{-1} is assigned to the overlapped vibrations of pyrrole and naphthalene stretching vibrations by analogy with those under 633 nm excitation.

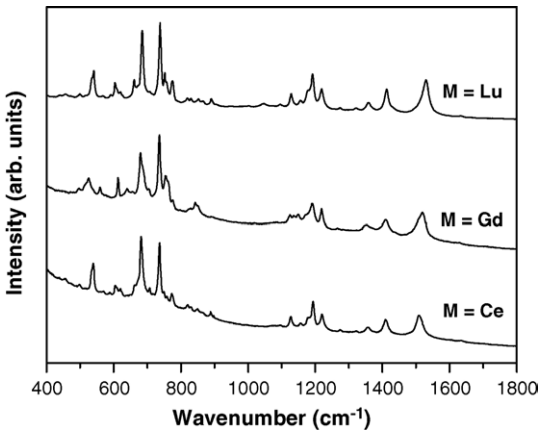

Fig. 16. Raman spectra of M[Nc(tBu)$_4$]$_2$ (M = Ce, Gd, Lu) Lu with excitation at 785 nm recorded on a few grains of the solid sample.

Under 785 nm laser line excitation, the vibrations at 681–685 cm^{-1} assigned to the Nc breathings, 1357–1361 cm^{-1} due to the naphthalene stretching vibrations, 1409–1413 cm^{-1} attributed to the isoindole stretching vibrations, and 1517–1530 cm^{-1} contributed from the aza stretch in the Raman spectra of M^{III}[Nc(tBu)$_4$]$_2$ are shifted to higher energy along with the ionic radius contraction. A linear correlation exists between the wavenumber of the aza stretching vibrations at ca. 1530 cm^{-1} and the tervalent rare earth ionic radii, as shown in Fig. S7 (Supplementary data). As can be seen from this figure, the datum for Ce fits well with the linear relationship established between the ionic radius of M^{III} and the frequencies of the aza stretching vibrations, demonstrating the tervalent valence state of cerium in Ce[Nc(tBu)$_4$]$_2$ from the Raman spectroscopic viewpoint.

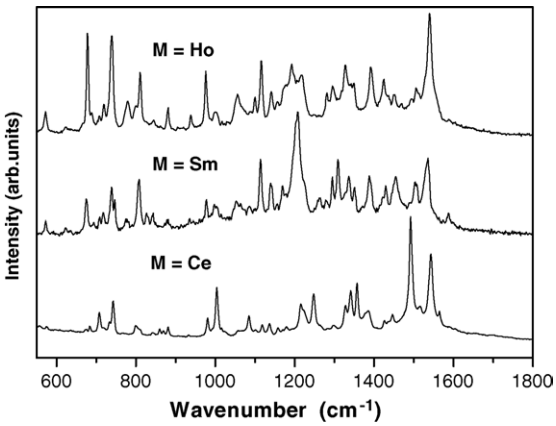

Fig. 17. Raman spectra of M(TClPP)(Pc) (M = Ce, Sm, Ho) with excitation 633 nm recorded on a few grains of the solid sample.

5.6. Raman spectra of M(TClPP)(Pc) [18]

As was noted in the previous work of Tran-Thi et al. on the mixed (porphyrinato)(phthalocyaninato) analogues M(TPP)(Pc) [38], the Raman spectra of these mixed ring rare earth compounds are dominated by the phthalocyanine contribution when exciting laser line of 1064 nm is employed. This is also true for complexes M(TClPP)(Pc) under the excitation using laser line of 633 and 785 nm because the phthalocyanine Q absorption bands located near 670 nm are in closer resonance with the laser source than are the porphyrin Q bands at ca. 550 nm, and the latter are only one-tenth as strong as the former.

Figs. 17 and 18 compare the Raman spectra for two tervalent rare earth compounds M(TClPP)(Pc) (M = Sm, Ho) together with that of Ce(TClPP)(Pc), obtained with excitation at 633 and 785 nm, respectively. The spectra with excitation at both wavelengths display similar features in the region of 500–1600 cm^{-1} for the whole series of tervalent rare earth double-deckers from M = La to Lu because of the similar electronic absorption characteristics of M^{III}(TClPP)(Pc) (M = Y, La–Lu except Ce and Pm) [50]. The close resemblance of the characteristic features of the Raman spectra of M(TClPP)(Pc) to those of respective $M(Pc)_2$ [12,19] excited at the same frequency, undoubtedly verifies the dominant contribution from the phthalocyanine ring to the Raman spectra of M(TClPP)(Pc). Groups of characteristic phthalocyanine vibrations have thus been similarly distinguished and attributed [18].

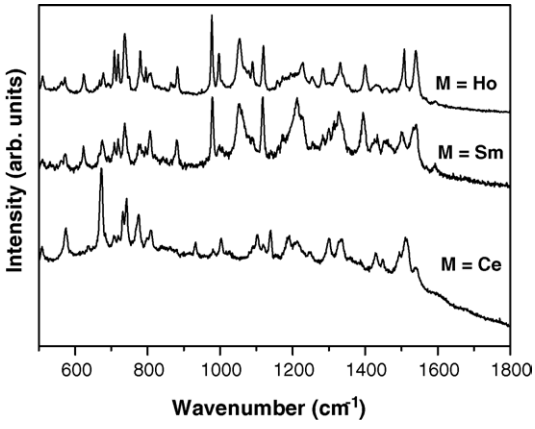

Fig. 18. Raman spectra of M(TClPP)(Pc) (M = Ce, Sm, Ho) with excitation 785 nm recorded on a few grains of the solid sample.

According to our theoretical research [39–41], the weak band at about 570 cm^{-1} and medium intense scattering at ca. 800 cm^{-1} are assigned to the central macrocycle (Pc) breathing vibrations. The intense band at 1340 cm^{-1} is contributed from the C=C stretching of the pyrrole groups and the C=C bonds of the benzene rings, also according to our calculations. The medium intense vibration at ca. 1307–1318 cm^{-1} also contains the contribution from stretching vibrations of both the C=C bonds of pyrrole rings and the C=C bonds in the benzene rings.

We now move to the cerium compound Ce(TClPP)(Pc), in which both the porphyrin and phthalocyanine rings exist as dianions despite the XANES results suggesting a valence state intermediate between III and IV for the cerium [62]. This compound, which can best be described as Ce(TClPP^{2-})(Pc^{2-}), shows a different Raman spectrum from those of the rest of the series. The close similarity in the spectra between Ce(TClPP)(Pc) displayed in Fig. 17 and $Ce(Pc)_2$ [19] under the same laser excitation, 633 nm, again reveals the dominant contribution of Pc^{2-} to the Raman characteristics of Ce(TClPP)(Pc). The marker Raman band of Pc^{2-} in the Raman spectrum of Ce(TClPP)(Pc) is observed at 1492 cm^{-1} as the strongest scattering. This is in strong contrast to the very weak $Pc^{\bullet-}$ marker Raman band observed for M^{III}(TClPP)(Pc) at 1510–1519 cm^{-1}. It is worth mentioning that the Pc^{2-} marker Raman band of Ce(TClPP)(Pc) at 1492 cm^{-1} downshifts about 8 cm^{-1} compared with that in $Ce(Pc)_2$ but corresponds well with that in the triple-deckers $M_2(Por)_2(Pc)$ and $M_2(Por)(Pc)_2$ [12].

When exciting the Raman spectrum of Ce(TClPP)(Pc) with 785 nm laser line, the intense band at 1511 cm^{-1} with contribution from both pyrrole C=C and aza C=N stretches together with isoindole stretching vibrations is the marker Raman band of Pc^{2-}, which upshifts 19 cm^{-1} compared with the band at 1492 cm^{-1} under excitation at 633 nm.

5.7. Raman spectra of M(OEP)(Nc) [15]

As was noted above (Sections 5.1 and 5.6), the Raman spectra of the mixed (porphyrinato)(phthalocyaninato) rare earth compounds are dominated by the phthalocyanine contribution when exciting laser lines of 1064, 633, and 780 (785) nm are employed. It is thus reasonable to conclude that the Raman spectroscopic patterns of M(OEP)(Nc) as well as M(TBPP)(Nc) are also dominated by the contributions from naphthalocyanine due to the location of the naphthalocyanine Q bands at even longer wavelength (around 780 nm) than those of phthalocyanine.

Figs. S8 and S9 (Supplementary data) compare the Raman spectra of four compounds M(OEP)(Nc) (M = Ce, Pr, Gd, Yb) under excitation by 633 and 785 nm light, respectively. The assignments given for the observed Raman frequencies are restricted to characteristic fundamentals based on the normal

modes for phthalocyaninato, naphthalocyaninato, and especially bis(naphthalocyaninato) metal derivatives [12,14,30].

The Raman spectra with excitation at 633 and 785 nm display similar features in the region of 450–1650 cm^{-1} for the whole series from M = La to Lu, suggesting as expected that the electronic structure of the Nc fragment in this series of double-decker compounds is similar. The close resemblance of the characteristic features of the Raman spectra of M^{III}(OEP)(Nc) to those of respective $M^{III}[Nc(tBu)_4]_2$ [14] excited at the same frequency again verifies the dominant contributions from the naphthalocyanine ring to the Raman spectra of M(OEP)(Nc).

The cerium complex Ce(OEP)(Nc), in which the naphthalocyanine ligand exists in the dianion form Nc^{2-}, shows anomalous spectroscopic data when compared with those of the rest of the series. Therefore, it is reasonable to attribute the Raman characteristics of Ce(OEP)(Nc) mainly to Nc^{2-}. This is also the case for Ce(TBPP)(Nc) (see below) [16]. A comparison of the Raman spectrum of Ce(OEP)(Nc) with those of the rest of the series shows that although Ce(OEP)(Nc) contains most of the frequencies found in the other complexes, the relative intensities are clearly different. For instance, a strong band appears at 1398 cm^{-1} for Ce(OEP)(Nc) (Fig. S8 (Supplementary data)) corresponding to isoindole stretching, but for the other complexes, only a weak band at about 1400 cm^{-1} is observed. The Raman spectra of M^{III}(OEP)(Nc) ($M \neq Ce$) exhibit intense naphthalene stretching at ca. 1598 cm^{-1} together with a very weak shoulder around 1625 cm^{-1}, while in Ce(OEP)(Nc) the most intense peak is observed at 1550 cm^{-1}, which is assigned to the naphthalene stretching vibration. Moreover, a broad and weak band centered at 1507 cm^{-1} in the spectrum of Ce(OEP)(Nc) is attributed to the coupling of pyrrole C=C and aza C=N stretches overlapped with the isoindole stretches of naphthalocyanine dianion by comparison with the Raman characteristics of M^{III}(OEP)(Nc) and $M^{III}[Nc(tBu)_4]_2$ [14].

5.8. Raman spectra of M(TBPP)(Nc) [16]

The Raman spectra for M(TBPP)(Nc) have been recorded under excitation by 633 and 785 nm light, respectively. Three groups of characteristic naphthalocyanine vibrations could be clearly distinguished and the assignments for Raman spectroscopic frequencies of naphthalocyanine in M(TBPP)(Nc) are made based on the work of $M[Nc(tBu)_4]_2$ and M(OEP)(Nc) [14,15].

As expected, the Raman characteristics of M(TBPP)(Nc) are quite similar to those of M(OEP)(Nc) [40] with the same excitation. The slight shifts in corresponding vibration frequencies in the Raman spectra of M(TBPP)(Nc) and M(OEP)(Nc) are easily attributed to the slightly different ring–ring interaction between the naphthalocyanine and different kinds of porphyrin ligand in the two series of compounds. The close resemblance of the characteristic features of Raman spectra of M(TBPP)(Nc) to those of the respective $M[Nc(tBu)_4]_2$ excited at the same frequency, again verifies the dominant contributions from the naphthalocyanine ring to the Raman spectra of the former series.

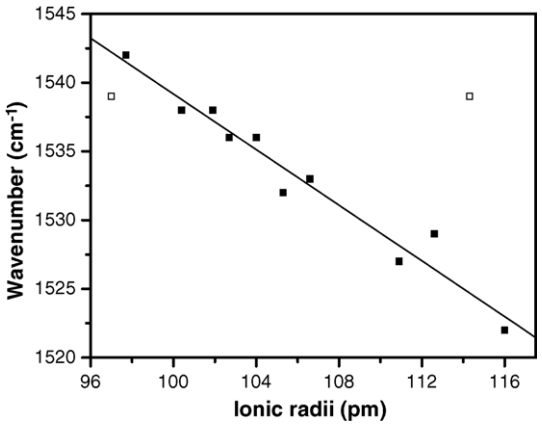

Fig. 19. Plot of wavenumber of the C=N aza stretching scattering of M(TBPP)(Nc) with excitation of 633 nm as a function of the ionic radius of M^{III}. The points for Ce^{IV} (97 pm) and Ce^{III} (114 pm) are shown with open squares.

As mentioned above, it has been verified for Ce(TBPP)(Nc) that the naphthalocyanine ligand can be regarded as the dianion Nc^{2-} [62]. However, the Raman spectroscopic features of Ce(TBPP)(Nc) with excitation at 633 nm laser line seem quite similar to those of the rest of the series. This appears difficult to understand at first glance as significant differences exist between the Raman characteristics of M^{III}(OEP)(Nc) and Ce(OEP)(Nc) under the same laser line excitation [15] but can be rationalized by the quite similar electronic absorption features of Ce(TBPP)(Nc) and M^{III}(TBPP)(Nc) especially in the region of 600–700 nm [56,62]. The marker Raman scattering of Nc^{2-} due to the isoindole stretching vibrations is shown as a relatively intense vibration at 1493 cm^{-1} in Ce(TBPP)(Nc). For other complexes of tervalent rare earths in this series from La to Lu, a medium intensity, relatively broad band assigned to the coupling of pyrrole and aza stretches was found at relatively higher energy, 1496–1507 cm^{-1}, which is actually a good marker Raman band of $Nc^{\bullet -}$ in M^{III}(TBPP)(Nc). The other marker Raman band of $Nc^{\bullet -}$ due to the aza group stretches appears as a weak broad peak at 1522 cm^{-1} for La(TBPP)(Nc), which moves to higher energy along with the rare earth contraction, to 1542 cm^{-1} for Lu(TBPP)(Nc). This peak should also have some contribution from the naphthalene stretching according to its broad appearance with a shoulder in the higher energy side. It is significant that neither 97 pm (cerium ionic radius in CeO_2) nor 114 pm (tervalent cerium ionic radius) places the frequency of the aza group stretch of Ce(TBPP)(Nc) on the linear relationship found for the M^{III}(TBPP)(Nc) (Fig. 19). This result is entirely in agreement with that derived from electronic absorption and electrochemical characteristics of this compound, confirming the intermediate valence state of cerium in Ce(TBPP)(Nc) [62].

Under excitation at 785 nm, in the Raman spectrum of Ce(TBPP)(Nc), the marker Raman peak of Nc^{2-} at 1497 cm^{-1} due to the coupling of pyrrole C=C and aza C=N stretches is the strongest Raman vibration. The $Nc^{\bullet -}$ marker Raman band due to the same vibrational modes in the spectra of M^{III}(TBPP)(Nc) blue-shifts to 1506–1509 cm^{-1} and appears as a weak or medium strong band.

6. Theoretical calculations on the IR spectra of phthalocyanine derivatives [39–41]

As noted above, assignments of the phthalocyanine vibrational bands had been made mainly from empirical comparison of experimental results among related compounds. These empirical assignments depending on the simple comparison method unavoidably lead to some doubtful assignments. To try to obviate this problem and to assist the assignments of the vibrational bands in the spectra of phthalocyanine-containing sandwich rare earth complexes, theoretical studies are thus necessary, by application of quantum chemistry calculations.

Recently, we have conducted theoretical investigations of the fully optimized structures and electronic properties of metal-free porphyrazine, phthalocyanine, and naphthalocyanine as well as their magnesium complexes based on density functional theory [41]. The infrared frequencies and intensities of H_2Pc, D_2Pc, and MgPc were further calculated using the 6-31G(d) basis set at the density functional B3LYP level [39,40]. Through comparison between the calculation results and experimental data, detailed assignments of N–H and N–M related vibrational modes are thus reached and some previous problematic assignments have been clarified.

For instance, the most intense band at 1005 cm^{-1} in the IR spectrum of H_2Pc has been regarded as a characteristic band of the metal-free H_2Pc and used as an effective marker to check the purity of synthesized metallophthalocyanine complexes [72]. This band was usually assigned to the N–H in-plane bending (IPB) or out-of-plane bending (OPB) mode as a result of comparing the IR spectra between metal-free phthalocyanine and its metal derivatives [71,72,77,88,89]. According to our calculated results of H_2Pc [39], the vibrational mode that shows the strongest absorption predicted at 1023 cm^{-1} should contribute to the absorption band at 1005 cm^{-1} in the IR spectrum of H_2Pc. The similar vibration mode for D_2Pc was predicted at 1022 cm^{-1} with similar intensity. These results agree very well with the conclusion of Sammes that the band at 1005 cm^{-1} was not affected either in position or in intensity upon deuteriation of the central protons in H_2Pc [90]. With the assistance of animated pictures, the C–N (pyrrole) in-plane bending vibrations at the two pyrrole rings which do not contain N–H bonds were found to play an important role in this vibration mode. As for the N–H in-plane bending mode previously assigned *empirically*, these are predicted at 1031 cm^{-1} for H_2Pc and 946.4 cm^{-1} for D_2Pc, respectively, according to our calculation results. Corresponding bands at 1043 and 961 cm^{-1} in the recorded IR spectra of H_2Pc and D_2Pc, respectively, should be assigned to this vibrational mode. On the basis of the present calculation results, we therefore re-assign the band at 1005 cm^{-1} in the IR spectrum of H_2Pc to the C–N (pyrrole) in-plane bending mode rather than N–H vibrations. Theoretical studies of the IR spectrum of Mg(Pc) revealed that the vibration mode at 1044 cm^{-1}, which is doubly-degenerate in nature, derives from the coupling of C–N (pyrrole) in-plane bending mode predicted at 1023 cm^{-1} and the N–H in-plane bending mode predicted at 1031 cm^{-1} for H_2Pc [40]. This clearly explains the disappearance of the band at 1005 cm^{-1} in the IR spectra of metallophthalocyanines, giving additional support to this assignment.

The other troublesome absorptions are the metal–ligand vibrations. There is no doubt that the band at 810–830 cm^{-1} for metallophthalocyanines, that is absent in metal-free phthalocyanine, should be assigned as the metal–ligand vibration. This is also in line with our calculation results. According to the calculations, two degenerate vibrations predicted at 792.2 cm^{-1}, which are considered to correspond to the band at 810–830 cm^{-1} in the IR spectra of M(Pc), are found to include M–N stretching and isoindole breathing and deformation. Corresponding vibrational modes for the metal-free phthalocyanine H_2Pc are predicted at 771.0 and 775.3 cm^{-1} [39]. However, the problem arises from the band at 888–919 cm^{-1} in the IR spectra of a series of metallophthalocyanines M(Pc) (M = Fe, Co, Ni, Cu, Zn, Pd, and Pt), which Kobayashi et al. attributed to the metal–ligand vibrations [77]. Kenn and Malerbi also assigned the similar IR band at 918 cm^{-1} for Pt(Pc) and the axially chloro-coordinated palladium phthalocyaninato compound Pd(Pc)Cl to metal–ligand vibration [78]. Clarisse and Riou, and Janczak observed similar vibrations at 886 cm^{-1} for $Lu(Pc)_2$ and $In(Pc)_2$ [72,88]. However, the observation of the IR band at 874 cm^{-1} for H_2Pc makes the attribution of these bands to metal–ligand vibrations controversial [39]. On the basis of our calculations, the degenerate vibrational modes predicted at 873.2 cm^{-1}, which are considered to correspond to the peak at 886–919 cm^{-1} observed in the IR spectra of M(Pc), have also been found to include M–N stretching and in-plane bending vibrations and isoindole deformation. This confirms the previous assignment of Kobayashi et al. and Kenn and Malerbi that the absorption at 888–919 cm^{-1} is due to the metal–ligand vibrations [77,78]. These two degenerate vibrational modes predicted at 873.2 cm^{-1} for Mg(Pc) are found to correspond with the modes predicted at 857.7 and 822.4 cm^{-1} for H_2Pc, respectively. The intensity of the mode predicted at 857.7 cm^{-1} for H_2Pc is much higher than that predicted at 771.0 cm^{-1}, thus a band was observed at 874 cm^{-1} instead of at ca. 810 cm^{-1} in the IR spectrum of H_2Pc. It is thus clear that both the bands at 888–919 and 810–830 cm^{-1} in the IR spectra of M(Pc) include M–N vibration, but vibration of the isoindole units contributes to the appearance of the 874 cm^{-1} band of H_2Pc.

As detailed in the above-described IR spectroscopic characteristics for the bis(phthalocyaninato) rare earth complexes [9], the band at 876–887 cm^{-1} of $M(Pc)_2$ was found to be metal size dependent. This gives further experimental support to the above-discussed assignment for this vibrational mode.

7. Conclusion

The IR and Raman spectra for several series of homoleptic bis(phthalocyaninato), heteroleptic bis(phthalocyaninato) and tris(phthalocyaninato), homoleptic bis(naphthalocyaninato), mixed (porphyrinato)(phthalocyaninato), and mixed (porphyrinato)(phthalocyaninato) complexes of the whole series of rare earth metals have been comparatively and systematically studied. The assignments of the vibrational bands of (na)phthalocyanines in these complexes have been proposed on

the basis of comparison with related monomeric phthalocyanine compounds and assisted by quantum chemistry calculations. The results reveal that the frequencies of pyrrole stretching, isoindole breathing, isoindole stretching vibrations, aza stretching vibrations and coupling of pyrrole and aza stretching vibrations are sensitive to the rare earth ionic size, which shift to higher energy along with the lanthanide contraction, indicating the increased ring–ring interaction in the same order. This body of work affords researchers in this field a large amount of comparative data with which to correlate new experimental results, and we hope this compilation and systematic discussion will assist the further development of the chemistry and technology of these fascinating sandwich complexes.

Acknowledgements

Financial support from the Natural Science Foundation of China (Grant Nos. 20325105, 20431010), National Ministry of Science and Technology of China (Grant No. 2001CB6105-07), Ministry of Education of China, Shandong University, and the Science Research Centre, Queensland University of Technology is gratefully acknowledged.

Appendix A. Supplementary data

Supplementary data associated with this article can be found, in the online version, at doi:10.1016/j.ccr.2005.09.009.

References

[1] A.B.P. Lever, C.C. Leznoff, Phthalocyanine: Properties and Applications, vols.1–4, VCH, New York, 1996.
[2] N.B. McKeown, Phthalocyanines Materials—Synthesis, Structure and Function, Cambridge University Press, New York, 1998.
[3] K.M. Kadish, K.M. Smith, R. Guilard, The Porphyrin Handbook, vols. 1–20, Academic Press, San Diego, 2000–2003.
[4] J. Jiang, K. Kasuga, D.P. Arnold, in: H.S. Nalwa (Ed.), Supramolecular Photo-sensitive and Electroactive Materials, Academic Press, New York, 2001, p. 113 (Chapter 2).
[5] D.K.P. Ng, J. Jiang, Chem. Soc. Rev. 26 (1997) 433.
[6] J. Jiang, W. Liu, D.P. Arnold, J. Porphyrins Phthalocyanines 7 (2003) 459.
[7] J. Jiang, D.P. Arnold, H. Yu, Polyhedron 18 (1999) 2129.
[8] X. Sun, M. Bao, N. Pan, X. Cui, D.P. Arnold, J. Jiang, Aust. J. Chem. 55 (2002) 587.
[9] F. Lu, M. Bao, C. Ma, X. Zhang, D.P. Arnold, J. Jiang, Spectrochim. Acta Part A 59 (2003) 3273.
[10] M. Bao, N. Pan, C. Ma, D.P. Arnold, J. Jiang, Vib. Spectrosc. 32 (2003) 175.
[11] W. Su, M. Bao, J. Jiang, Vib. Spectrosc. 39 (2005) 186.
[12] J. Jiang, L. Rintoul, D.P. Arnold, Polyhedron 19 (2000) 1381.
[13] J. Jiang, U. Cornelisson, D.P. Arnold, X. Sun, H. Homborg, Polyhedron 20 (2001) 557.
[14] N. Pan, L. Rintoul, D.P. Arnold, J. Jiang, Polyhedron 21 (2002) 1905.
[15] Y. Bian, L. Rintoul, D.P. Arnold, N. Pan, J. Jiang, Vib. Spectrosc. 31 (2003) 173.
[16] X. Sun, L. Rintoul, Y. Bian, D.P. Arnold, R. Wang, J. Jiang, J. Raman Spectrosc. 34 (2003) 306.
[17] M. Bao, Y. Bian, L. Rintoul, R. Wang, D.P. Arnold, C. Ma, J. Jiang, Vib. Spectrosc. 34 (2004) 283.
[18] F. Lu, L. Rintoul, X. Sun, D.P. Arnold, X. Zhang, J. Jiang, J. Raman Spectrosc. 35 (2004) 860.
[19] M. Bao, R. Wang, L. Rintoul, Q. Liu, D.P. Arnold, C. Ma, J. Jiang, Polyhedron, in press.
[20] M. Bao, R. Wang, L. Rintoul, D.P. Arnold, J. Jiang, Vib. Spectrosc., in press.
[21] R. Aroca, R.E. Clavijo, C.A. Jennings, G.A. Kovacs, J.M. Duff, R.O. Loutfy, Spectrochim. Acta 45A (1989) 957.
[22] R.E. Clavijo, D. Battisti, R. Aroca, G.J. Kovacs, C.A. Jennings, Langmuir 8 (1992) 113.
[23] M.L.R. Mendez, Y. Khoussed, J. Souto, J. Sarabia, R. Aroca, J.A. de Saja, Sens. Actuators B 18–19 (1994) 89.
[24] R. Aroca, E. Johnson, Langmuir 8 (1992) 3137.
[25] M.L. Rodriguez-Mendez, R. Aroca, J.A. Desaja, Spectrochim. Acta 49A (1993) 965.
[26] R.E. Clavijo, D. Battisti, R. Aroca, G.J. Kovacs, C.A. Jennings, Langmuir 8 (1992) 113.
[27] J. Souto, L. Tomilova, R. Aroca, Langmuir 8 (1992) 942.
[28] M.L. Rodriguez-Mendez, R. Aroca, Chem. Mater. 5 (1993) 933.
[29] J. Souto, R. Aroca, J. Raman Spectrosc. 22 (1991) 349.
[30] C. Jennings, R. Aroca, A.M. Hor, J.A. DeSaja, Chem. Mater. 7 (1995) 118.
[31] G. Ostendorp, H. Homborg, Z. Anorg. Allg. Chem. 622 (1996) 873.
[32] G. Ostendorp, H. Homborg, Z. Anorg. Allg. Chem. 622 (1996) 1358.
[33] M.S. Haghighi, A. Franken, H. Homborg, Z. Naturforsch. 49b (1994) 812.
[34] M.S. Haghighi, H. Homborg, Z. Anorg. Allg. Chem. 620 (1994) 1278.
[35] M.S. Haghighi, G. Peters, H. Homborg, Z. Anorg. Allg. Chem. 620 (1994) 1285.
[36] G. Ostendorp, H. Homborg, Z. Anorg. Allg. Chem. 622 (1996) 1222.
[37] G. Ostendorp, H. Homborg, Z. Naturforsch. 50b (1995) 1200.
[38] T.H. Tran-Thi, T.A. Mattioli, D. Chabach, A. De Cian, R. Weiss, J. Phys. Chem. 98 (1994) 8279.
[39] X. Zhang, Y. Zhang, J. Jiang, Vib. Spectrosc. 33 (2003) 153.
[40] X. Zhang, Y. Zhang, J. Jiang, Spectrochim. Acta Part A 60 (2004) 2195.
[41] X. Zhang, Y. Zhang, J. Jiang, J. Mol. Struct.: Theochem. 673 (2004) 103.
[42] J. Jiang, R.C.W. Liu, T.C.W. Mak, D.K.P. Ng, T.W.D. Chan, Polyhedron 16 (1997) 515.
[43] J. Jiang, J. Xie, M.T.M. Choi, D.K.P. Ng, J. Porphyrins Phthalocyanines 3 (1999) 322.
[44] J. Jiang, J. Xie, D.K.P. Ng, Y. Yan, Mol. Cryst. Liq. Cryst. 337 (1999) 385.
[45] W. Liu, J. Jiang, D. Du, D.P. Arnold, Aust. J. Chem. 53 (2000) 131.
[46] J. Jiang, T.C.W. Mak, D.K.P. Ng, Chem. Ber. 129 (1996) 933.
[47] J. Jiang, R.L.C. Lau, T.W.D. Chan, T.C.W. Mak, D.K.P. Ng, Inorg. Chim. Acta 155 (1997) 59.
[48] R.L.C. Lau, J. Jiang, D.K.P. Ng, T.W.D. Chan, J. Am. Soc. Mass Spectrosc. 8 (1997) 161.
[49] J. Jiang, W. Liu, W.-F. Law, D.K.P. Ng, Inorg. Chim. Acta 268 (1998) 49.
[50] F. Lu, X. Sun, R. Li, D. Liang, P. Zhu, X. Zhang, C.-F. Choi, D.K.P. Ng, T. Fukuda, N. Kobayashi, J. Jiang, New J. Chem. 28 (2004) 1116.
[51] X. Sun, R. Li, D. Wang, J. Dou, P. Zhu, F. Lu, C. Ma, D.K.P. Ng, N. Kobayashi, J. Jiang, Eur. J. Inorg. Chem. (2004) 3806.
[52] X. Sun, X. Cui, D.P. Arnold, M.T.M. Choi, D.K.P. Ng, J. Jiang, Eur. J. Inorg. Chem. (2003) 1555.
[53] Y. Bian, R. Wang, J. Jiang, C.-H. Lee, J. Wang, D.K.P. Ng, Chem. Commun. (2003) 1194.
[54] Y. Bian, R. Wang, D. Wang, P. Zhu, R. Li, J. Dou, W. Liu, C.-F. Choi, C. Ma, D.K.P. Ng, J. Jiang, Helv. Chim. Acta 87 (2004) 2581.
[55] J. Jiang, Y. Bian, F. Furuya, W. Liu, M.T.M. Choi, N. Kobayashi, H.-W. Li, Q. Yang, T.C.W. Mak, D.K.P. Ng, Chem. Eur. J. 7 (2001) 5059.
[56] J. Jiang, W. Liu, K.-L. Cheng, K.-W. Poon, D.K.P. Ng, Eur. J. Inorg. Chem. (2001) 413.
[57] F. Furuya, N. Kobayashi, Y. Bian, J. Jiang, Chem. Lett. (2001) 944.
[58] Y. Bian, D. Wang, R. Wang, L. Wen, L. Dou, D. Zhao, D.K.P. Ng, J. Jiang, New J. Chem. 27 (2003) 844.

[59] J. Jiang, D. Du, M.T.M. Choi, J. Xie, D.K.P. Ng, Chem. Lett. (1999) 261.
[60] J. Jiang, W. Liu, K.-W. Poon, D.P. Arnold, D.K.P. Ng, Eur. J. Inorg. Chem. (2000) 205.
[61] T. Nyokong, F. Furuya, N. Kobayashi, W. Liu, D. Du, J. Jiang, Inorg. Chem. 39 (2000) 128.
[62] Y. Bian, J. Jiang, Y. Tao, M.T.M. Choi, R. Li, A.C.H. Ng, P. Zhu, N. Pan, X. Sun, D.P. Arnold, Z. Zhou, H.-W. Li, T.C.W. Mak, D.P.K. Ng, J. Am. Chem. Soc. 125 (2003) 12257.
[63] P. Zhu, N. Pan, R. Li, J. Dou, Y. Zhang, D.Y.Y. Cheng, D. Wang, D.K.P. Ng, J. Jiang, Chem. Eur. J. 11 (2005) 1425.
[64] W. Liu, J. Jiang, D.P. Arnold, N. Pan, Inorg. Chim. Acta 310 (2000) 140.
[65] D.P. Arnold, J. Jiang, J. Phys. Chem. A 105 (2001) 7525.
[66] Y. Bian, L. Li, D. Wang, C.-F. Choi, D.Y.Y. Cheng, P. Zhu, R. Li, J. Dou, R. Wang, N. Pan, C. Ma, D.K.P. Ng, N. Kobayashi, J. Jiang, Eur. J. Inorg. Chem. (2005) 2612.
[67] A.G. Gurek, V. Ahsen, D. Luneau, J. Pecaut, Inorg. Chem. 40 (2001) 4793.
[68] L.A. Lapkina, Y. Gorbunova, S.E. Nefedov, A.V. Tsivadze, Russ. Chem. Bull. 52 (2003) 1.
[69] (a) R. Wang, R. Li, Y. Bian, C.-F. Choi, D.K.P. Ng, J. Dou, D. Wang, P. Zhu, C. Ma, R.D. Hartnell, D.P. Arnold, J. Jiang, Chem. Eur. J., in press;
(b) N. Sheng, R. Li, P. Zhu, W. Su, D.K.P. Ng, M. Bao, T. Takami, X. Li, J. Jiang, manuscript in preparation.
[70] S.I. Troyanov, L.A. Lapkina, V.E. Larchenko, A. Yu Tsivadze, Dokl. Akad. Nauk 367 (5) (1999) 644 (in Russian);
S.I. Troyanov, L.A. Lapkina, V.E. Larchenko, A. Yu Tsivadze, Doklady Chem. 367 (4–6) (1999) (in English).
[71] H.F. Shurvell, L. Pinzuti, Can. J. Chem. 44 (1966) 125.
[72] C. Clarisse, M.T. Riou, Inorg. Chim. Acta 130 (1987) 139.
[73] H. Hückstädt, A. Tuta, M. Göldner, U. Cornelissen, H. Homborg, Z. Anorg. Allg. Chem. 627 (2001) 485.
[74] K.M. Kadish, G. Moninot, Y. Hu, D. Dubois, A. Ibnlfassi, J.-M. Barbe, R. Guilard, J. Am. Chem. Soc. 115 (1993) 8153.
[75] R. Guilard, J.-M. Barbe, A. Ibnlfassi, A. Zirneh, V.A. Adamian, K.M. Kadish, Inorg. Chem. 34 (1995) 1472.
[76] H. Isago, M. Shimoda, Chem. Lett. (1992) 147.
[77] T. Kobayashi, F. Kurosawa, N. Uyeda, E. Suito, Spectrochim. Acta 26A (1970) 1305.
[78] I.M. Kenn, B.W. Malerbi, J. Inorg. Nucl. Chem. 27 (1965) 1311.
[79] M.L. Kaplan, A.J. Lovinger, W.D. Reents Jr., P.H. Schmidt, Mol. Cryst. Liq. Cryst. 12 (1984) 345.
[80] H. Yanagi, T. Kouzeki, M. Ashida, T. Noguchi, A. Manivannan, K. Hashimoto, A. Fujishima, J. Appl. Phys. 71 (1992) 5146.
[81] H. Yanagi, T. Kouzeki, M. Ashida, J. Appl. Phys. 73 (1993) 3812.
[82] R.E. Clavijo C., M.M. Campos-Vallette, M. Saavedra S., A. Alvarado, G. Diaz F., Vib. Spectrosc. 14 (1997) 79.
[83] M. Saavedra S., F. Mendizabal, M.M. Campos-Vallette, R.E. Clavijo C., G. Diaz F., Vib. Spectrosc. 18 (1998) 25.
[84] E.A. Carrasco F., M.M. Campos-Vallette, M. Saavedra S., G. Diaz F., R.E. Clavijo C., J.V. Garcia-Ramos, S. Sanchez-Cortes, Vib. Spectrosc. 26 (2001) 201.
[85] P. Zhu, N. Pan, C. Ma, X. Sun, D.P. Arnold, J. Jiang, Eur. J. Inorg. Chem. (2004) 518.
[86] M. Bao, G. Song, F. Lu, M. Bai, J. Jiang, Chin. J. Inorg. Chem. 20 (2004) 1203 (in Chinese).
[87] C.A. Melendres, V.A. Maroni, J. Raman Spectrosc. 15 (1984) 319.
[88] J. Janczak, Polish J. Chem. 72 (1998) 1871.
[89] B. Stymne, F.X. Sauvage, G. Wettermark, Spectrochim. Acta 35A (1979) 1195.
[90] M.P. Sammes, J. Chem. Soc. Perkin II (1972) 160.